UNIVERSITY OF GAZIANTEP

GRADUATE SCHOOL OF

NATURAL AND APPLIED SCIENCES

THE EFFECT OF HEATING RATE ON THE DOSE DEPENDENCE AND THERMOLUMINESCENCE CHARACTERISTICS OF $CaSO_4$:Dy (TLD-900)

M. SC. THESIS

IN

ENGINEERING PHYSICS

BY

KARWAN FAEEED MAJEED

SEPTEMBER 2014

The Effect of Heating Rate on The Dose Dependence and Thermoluminescence Characteristics of $CaSO_4$:Dy (TLD-900)

M. Sc. Thesis

In

Engineering physics

University of Gaziantep

Supervisor

Assist. Prof Dr. Vural Emir KAFADAR

by

Karwan Fareed MAJEED

September 2014

© 2014 [Karwan Fareed MAJEED]

T. C.

UNIVERSITY OF GAZIANTEP
GRADUATE SCHOOL OF NATURAL AND APPLIED SCIENCES
ENGINEERING PHYSICS DEPARTMENT

Name of the thesis: The effect of heating rate on the dose dependence and thermoluminescence characteristics of CaSO4: Dy (TLD-900)

Name of the student: Karwan Fareed MAJEED

Exam date: 30.09.2014

Approval of the Graduate School of Natural and Applied Sciences

Assoc. Prof. Dr. Metin BEDİR
Director

I certify that this thesis satisfies all the requirements as a thesis for the degree of Master of Science.

Prof. Dr. A. Necmeddin YAZICI
Head of Department

This is to certify that we have read this thesis and that in our opinion it is fully adequate, in scope and quality, as a thesis for the degree of Master of Science.

Assist. Prof Dr. Vural Emir KAFADAR
Supervisor

Examining Committee Members **signature**

Assist. Prof Dr. Vural E KAFADAR ----------

Assist. Prof Dr. R. Güler YILDIRIM ----------

Assist. Prof Dr. M.Yakup HACİİBRAHİMOĞLU ----------

hereby declare that all information in this document has been obtained and presented in accordance with academic rules and ethical conduct. I also declare that, as required by these rules and conduct, I have fully cited and referenced all material and results that are not original to this work.

Karwan Fareed MAJEED

ABSTRACT

THE EFFECT OF HEATING RATE ON THE DOSE DEPENDENCE AND THERMOLUMINESCENCE CHARACTERISTIC OF $CaSO_4$: Dy (TLD-900)

MAJEED, Karwan Fareed

M.Sc. in Engineering Physics

Supervisor: Assist. Prof. Dr. Vural E. KAFADAR

September 2014

61 pages

$CaSO_4$:Dy (TLD-900) doped with dysprosium, having an effective number of 15.5, is a solid state dosimeter and it has been used in the investigation for detecting and measuring radiation for the past two decades. In the given study, the effect of heating rate on the dose dependence and thermoluminescence characteristics of TLD-900 has been investigated by using the dose response function f (D) at different linear heating rates between 1 ^{o}C/s and 10 ^{o}C/s. It is observed that, the peak temperature of the main dosimetric glow peak (P2) shifts to higher temperature sides and the integrated peak area decreases by about 50% as the heating rate increases due to thermal quenching.

Keywords: CaSO4: Dy (TLD-900); heating rate; dose response function f (D); thermal quenching

ÖZET

ISITMA HIZININ $CaSO_4$: Dy (TLD-900) 'ÜN TERMOLÜMİNESANS KARAKTERİSİĞİ VE DOZ BAĞLILIĞINA ETKİSİNİN İNCELENMESİ

MAJEED, Karwan Fareed

Yüksek Lisans Tezi, Fizik Mühendisliği Bölümü

Tez Yöneticisi: Y. Doç.Dr. Vural E. KAFADAR

Eylül 2014

61 sayfa

Disporsiyum katkılanmış $CaSO_4$:Dy (TLD-900) etkin atom numarası 15,5 olan ve özellikle son 20 yıldır iyonize radyasyonun tespit edilmesi ve ölçülmesinde kullanılan bir katı hal dozimetresidir. Bu çalışmada, ısıtma hızının TLD-900 kristalinin ışıma eğrileri üzerine etkisi doz-cevap fonksiyonu ve doğrusallık fonksiyonu f(D) kullanılarak araştırılmıştır. Doz-cevap fonksiyonu, 1 ^{o}C/s and 10 ^{o}C/s arasinda lineer ısıtma hızları kullanılarak elde edilmiştir. Elde edilen sonuçlar ana dozimetrik pikin tepe sıcaklığının (P2) ısıtma hızının artmasıyla yüksek sıcaklıklara doğru kaydığı ve ışıldama eğrisi altındaki toplam alanın termal sönüme bağlı olarak 50 % oranında azaldığı gözlenmiştir.

Anahtar Kelimeler: CaSO4:Dy (TLD-900); ısıtma hızı; doz-cevap fonksiyonu f(D);termal sönüm

To my family

Dedicate this modest effort

Karwan

ACKNOWLEDGEMENT

I would like to express my heartfelt thanks and deep gratitude to my supervisor Assist. Prof. Dr. VURAL EMIR KAFADAR for the continuous support of my M.Sc, study and research, for his ongoing advice, encouragements, the great moral motivation, patience, brotherly treatment and insight throughout the writing of this research work.

My gratitude is due to the head and staff Engineering of the Physics Department in the College of Science for their assistant and support during the years of my study and research.

I extend my thanks and gratitude to Assist. Prof. Dr QUSAY ABDULWAHAB for everything difficult making easy for me.

Contents

LIST OF FIGURES

CHAPTER 1

INTRODUCTION

For nearly 35 years there have been activity significantly in the nuclear power industry, is no secret to one the increasing use of radiation in all fields, especially medical, and it was necessary to detect and assess the radiation detection and dose assessment has never been higher, and here come the role of Thermoluminescence dosimeters (TLD), the study of materials that emit light when heated after exposure to ionizing radiation, has been a mainstay of health physics professionals for over 55 years. During that time, TLD have been very valuable in monitoring the safety of radiation workers and performing environmental dose control. Although very accurate active radiation detectors are now available, TLD are small, inexpensive, and if the correct material is chosen, tissue equivalent. They can be used to detect gamma rays, x-ray, beta particles, and slow neutrons, and with suitable filters, can be used to determine the shallow and deep dose. Their biggest advantage is long-term. The possibility of spreading possible due to a power source being unnecessary until readout. This allows time efficient monitoring of typically uninhabited areas. In order to ensure accurate results from long deployments in diverse interior and exterior environments, However, various aspects of their performance must be examined.

Dosimetry is the measurement of absorbed dose of ionizing radiation by matter or tissue and is measured in the SI unit of gray (Gy) or Sievert (Sv); Where 1 Gy and 1 Sv are equal to 1 joule per kilogram. It is noted here that the non-SI units of rad (absorbed radiation dose; for the matter) and rem (Roentgen equivalent in man; for tissue) are still heavily used; their conversions are given by 1 Gy=100 rad and 1 Sv=100 rem. A dosimetry allows us directly or indirectly to measure exposure, kerma, absorbed or equipollent dose and associated rates of ionizing radiation. A dosimeter system consists of the actual dosimeter and a linked reader. A dosimetry is characterized by its accuracy and precision, linearity,

energy response, dose and dose rate dependence, spatial resolution and directional dependence.

It is well documented that even low doses of ionizing radiation can induce cancer. Thus, personal radiation monitoring, i.e. dosimetry applied to people, has become highly important in recent years as the number of potential radiation sources is ever increasing [1]. Radiation dosimetry measures the dose absorbing by the sample that is exposed to irradiation. Radiation dosimetry has three subgroups; personnel dosimetry, medical dosimetry and environmental dosimetry. Personnel dosimetry is used in areas where the persons are exposed to radiation; nuclear reactors, radiotherapy wings in hospitals and nuclear powered submarines or such. Therefore, the purpose of using personal dosimetry is to keep track of the radiation exposure level of the individual to avoid overt radiation based effects. The safe limits are determined by organizations such as the International Commission on Radiological Protection (ICRP). Besides, from the constant radiation exposure, there are accidental or incidental radiation exposures, which are also measured by personnel dosimetry. Personnel dosimetry has three subcategories; extremity dosimetry, whole-body dosimetry and tissue dosimetry. The first one focuses on body parts that are exposed to radiation, such as hands, arms or feet while the whole-body focuses on the tissue below the surface of the body or the critical organs. It measures the dose absorbed in these parts of the body by dealing with gamma and X rays (greater than 15 keV) and neutrons, which are penetrating rays. Tissue dosimetry, which is also called skin dose, measures the dose absorbed by the skin. However, rather than dealing with penetrating radiation, it focuses on non-penetrating radiation, such as beta particles or <15 KeV X rays.

In order for these measurements to be done, a thermoluminescence dosimetry (TLD) material that is equivalent to the human tissue is needed. The TLD material should absorb the same dose or the amount of radiation as the human tissue would do in the same area within the same radiation levels. Medical dosimetry intends to measure the effects of a TLD that is placed in the appropriate places within the human body. By doing so, before exposing the patient, to ionizing radiations for treatment procedures or diagnosis, measurements can be made upon these TLD. From the data obtained, possible additional treatments or dose control can be implemented. It is impossible to do so by means of other than radiation dosimeter.

The major variables determining patient doses include imaging modality, technical factors and in the case of fluoroscopy, beam time. In addition to these factors, the size of the patient is also a determining factor. Medical dosimetry has two categories; diagnostic radiology and radiotherapy.

The radiation used here may be X-rays (10 keV level), gamma rays, beta particles, protons and other heavy particles and neutron. Again, the TLD material needs to be tissue equivalent and highly sensitive. The latter is needed for measurements done in laboratory conditions that require the possible smallest size of TLD material. Other than these properties, the TLD should not be toxic. Recommended diagnostic reference levels for medical imaging modalities have been published by the ICRP. Environmental dosimetry deals with the radiation present in the environment due to humankind. Due to applications like nuclear power stations, waste disposals, usage or processing of nuclear fuels and disastrous nuclear power plant malfunctions introduces high levels of radiation into the environment. Therefore, it's become essential to monitor the radiation released to the environment continuously. TLD are used for environmental dosimetry applications. However, the performance criteria for TLD in this application are different from those required for personnel monitoring. They are still needed to be highly sensitive, more preferably extremely sensitive and this time it is not essential for TLD to be tissue equivalent. Because the environment is exposed to radiation for a long time continuously, environmental dosimetry measures the values within a long period.

Therefore, the TLD should be structurally intact and stable in the long term. In recent years, with the help of cutting edge technological innovations, space flight with astronauts has been possible. Radiation exists in space and since there is no more an atmosphere to protect from galactic cosmic rays, it is important to measure the radiation at these space flights. Besides, from the astronauts on board, the radiation is also harmful for the digital equipment of the vehicles. The radiation sources are galactic cosmic rays of which the main component is high-energy protons and heavy charged particles from the solar wind. In order to measure the effects of these radiation sources, TLD are used. Thermoluminescence is used in age determining processes of materials, as it became an established method of age determination. A famous scientist, Daniels and his coworkers are

the first to suggest the use of thermoluminescence for this purpose. Thermoluminescence was used for age determination of rock formations, however;it was not used for archeological dating until natural thermoluminescence was found in ancient samples. Due to the effects of heat on thermoluminescence, thermoluminescence of the pots diminished to zero during its bakery [2]. All the branches of science, industry and medicine, where ionizing radiation is used, require exact dosimetric equipment for radiation dose monitoring. There are two different tasks, personnel and environmental dosimetry. Both tasks are best implemented using thermoluminescence dosimeters (TLD). The TLD has the following advantages:

- High sensitivity to ionizing radiation.
- Low non-radiation effects on dose storage and readout.
- Low dependence of thermoluminescence yield on the radiation dose rate.
- Wide measuring range (from 10–6 Sv to 105 Sv).
- Storage of information for long time (years) without losses.
- Good measurement reproducibility.
- High radiation stability.
- Thermal and chemical stability.
- Reusability.
- Possibility of proper TLD choice for a certain task, including a good tissue The equivalence for personnel dosimetry and predictable output depends on exciting photon (X-ray) energy.
- Small size.
- Low production cost, good synthesis repeatability.
- Possibility of selective radiation dosimetry.

Thermoluminescence may be broadly defined as the emission of light when solid is heated to a temperature below that of incandescence, and in general the properties noted, are a result of crystal imperfections. All crystals have defects, which may be due to a vacancy at one of the lattice points, an impurity atom a lattice point or an interstitial atom or ion in the lattice structure. Regardless of type, the presence of imperfections will introduce new energy levels into the normal lattice energy bands. It is possible, that some of the energy levels will

constitute metastable states and be able to trap whether electrons or holes for extended periods of time. The excitation can be stored also in some metastable excited charge-transfer states which will appear when impurity ion demonstrates a well-pronounced covalent bond with the legends. Many different natural minerals and synthetic inorganic compounds demonstrate the thermoluminescence phenomenon, however, only a small part of them satisfy the requirements mentioned above for TLD. The mechanism of excitation energy transformation in the output light is one of the most crucial points in the luminescent materials designing. Both the threshold of radiation dose detection and accuracy of measurements depends on the efficiency of energy transformation in TLD, or TLD sensitivity. Only a Small fraction of absorbed energy of ionizing radiation is released later at TLD annealing in the form of thermoluminescence light output. There are inevitable losses at energy transformation in the TLD [3-5]. Thermoluminescence (TL) can be defined as the emission of light from a semiconductor or an insulator when it is heated, due to the previous absorption of energy from irradiation. This is not to be fused with the light spontaneously emitted from a substance when it is heated to incandescence. Thermoluminescence is the thermally stimulated emission of light following the previous absorption of energy from radiation. The emitted light is recorded as the intensity vs. temperature in the shape of one or more TL peaks. Thermoluminescence is the thermally stimulated emission of light from an insulator or a semiconductor following the previous absorption of energy from ionizing radiation. The thermoluminescence process can be understood in terms of the band structure model of insulators. The phenomenon of thermoluminescence (TL) of minerals was known empirically as early as 1663.

It was in this year that Sir Robert Boyle reported to the Royal Society about "Experiments and Considerations upon Colors with Observations on Diamond That Shines in the Dark" (1663) and described how, upon warming a diamond in contact with his body in the dark, he saw a flash. This reflects the definition of thermoluminescence. Not only diamonds, but a large number of minerals emit light energy upon warming. Well known examples are quartz, feldspar calcite and flint (sedimentary cryptocrystalline form of the mineral quartz) [6]. The thermoluminescence is a process differs from the light emitted spontaneously from

a substance when it is heated to incandescence. Say over 200°C (or at high temperatures) a solid substance emits (infra-red) radiation of which the intensity of it increases with increasing temperature. This process is called (thermal) or (black body radiation).

In thermoluminescence phenomena can be found the three essential ingredients necessary for the productions of thermoluminescence. Firstly, the material must be an insulator or a semiconductor-metal do not exhibit luminescent properties. Secondly, the material must have at some time absorbed energy during exposure to radiation. Thirdly, the luminescence emission is triggered by heating the material. In addition, there is one important property of thermoluminescence which cannot be inferred from this statement as it stands at present. It is a particular characteristic of thermoluminescence that, once heated to excite the light emission, the material cannot be made to emit thermoluminescence again by simply cooling the specimen and reheating. In order to re-exhibit luminescence the material has to be re- exposed to radiation, whereupon raising the temperature will once again produce light emission. The fundamental principles which govern the production of thermoluminescence are essentially the same as those which govern all luminescence process, and in this way thermoluminescence is merely one of a large family of luminescence phenomena [7].

Thermoluminescence (TL) is observed under condition of steadily increasing temperature. In the usual TL experiments, the TL systems are irradiated at room temperature (RT) and later heated through a temperature range where the luminescence is bright until a temperature level at which all the charges have been thermally excited out of their metastable levels and the luminescence completely disappears. If the light emission is plotted as a function of temperature or time the graphs is known as glow-curve [8]. Thermoluminescence method is a relative complex process since it involves a trap and a luminescence center. The substances like insulators or semiconductors is exposed to ionizing radiation at room or low temperature, electrons are released from the valence band to the conduction band. This leaves a hole in the valence band. Both types of carriers become mobile in their respective bands until they recombine or until they are trapped in lattice imperfections in the crystalline solids. These lattice imperfections play very crucial role in the TL process. The trapped electrons may remain for a long period when

the crystals are stored at room temperature or they can be released due to the sufficient energy given to the electrons when the crystal is heated. These electrons may move in the crystalline solid until they recombine with suitable recombination centers that contain hole with the emission of TL light. This process of light emission by thermal stimulation from a crystalline solid after irradiations is called as “thermally stimulated process” or simply “thermoluminescence”. This thermally stimulated light contains information about the trap structure of the TL material and its previous exposure to the ionizing radiations [2].

CHAPTER 2

REVIEW OF LITERATURE

2.1 Thermoluminescence Mechanism

Thermoluminescence can be explained in two stages. The first phase is the change of the system from equilibrium to a metastable state by energy absorption in the UV or ionizing radiation. Then the second stage is a relaxation of the system back to the equilibrium with energy release such as light with the help of thermal stimulation. Thus, thermoluminescence (TL) is the thermally stimulated emission of light following the previous absorption of energy from radiation [9].

2.2 Energy Storage

There are two ways for the stability of this absorbed energy: electron excitation and displacement damage. At the end of both processes, radiation-induced defects are formed in the material structure. Radiation-induced defects are localized electronic states occupied by non-equilibrium concentration of electrons [10]. Before irradiation, materials have localized electron energy states and after irradiation, some of these states are occupied by a non-equilibrium concentration of electrons. Therefore, these occupied states are called radiation-induced defects. According to McKeever, when investigations take into consideration, they show that the cause of defect creation is electronic excitation rather than non-ionizing displacement damage [9]. In addition, there exists a mid-gap state caused by defects which may be created by pre-existing impurities or radiation induced defects. This gap is found between two energy bands; i.e. conduction band and valence band. The valence band is the outermost energy level and contains electron-hole pairs in the ground state of the solid. On the other hand; in the conduction band, electrons are free to move and have the ability to produce electric current. According to thermoluminescence phenomena, it is supposed that there are two kinds of imperfections called electron traps and hole trap in the

crystal which are localized at mid gap states. In the mid- cap, the electron trap is believed close to the conduction band and the hole trap is far from the valence band

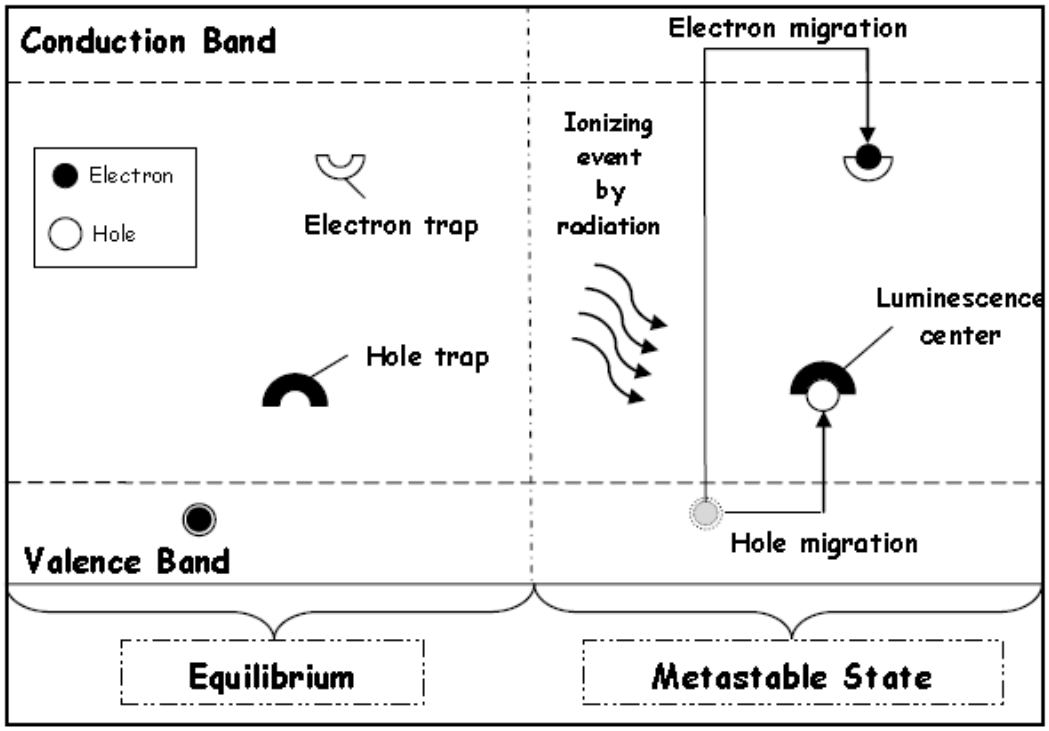

Figure 2.1 Energy-level diagram of the energy storage stage for thermoluminescence processes [10].

Figure 2.1 illustrates the energy storage mechanism. After irradiation, the electrons pass from the valence band to the conduction band and the hole becomes a positively charged area in the valence band. When the electron reaches the conduction band, electron find its way into an electron trap and hole occupies its associated trap. Hole traps are called luminescence center in this process.

2.3 Energy Release

Excitation with an increase in temperature or giving light, results in the release of the stored energy. In addition, the state of the material changes from metastable to ground. When heat is increased, the trapped electron trapped in the electron trap is released to conduction band. Afterward this electron is free to re-trap or recombine with the hole found in the hole trap. The recombination of the electron with the

hole in the hole trap results in the emission of photons. In this case hole trap is called as recombination centers [11].

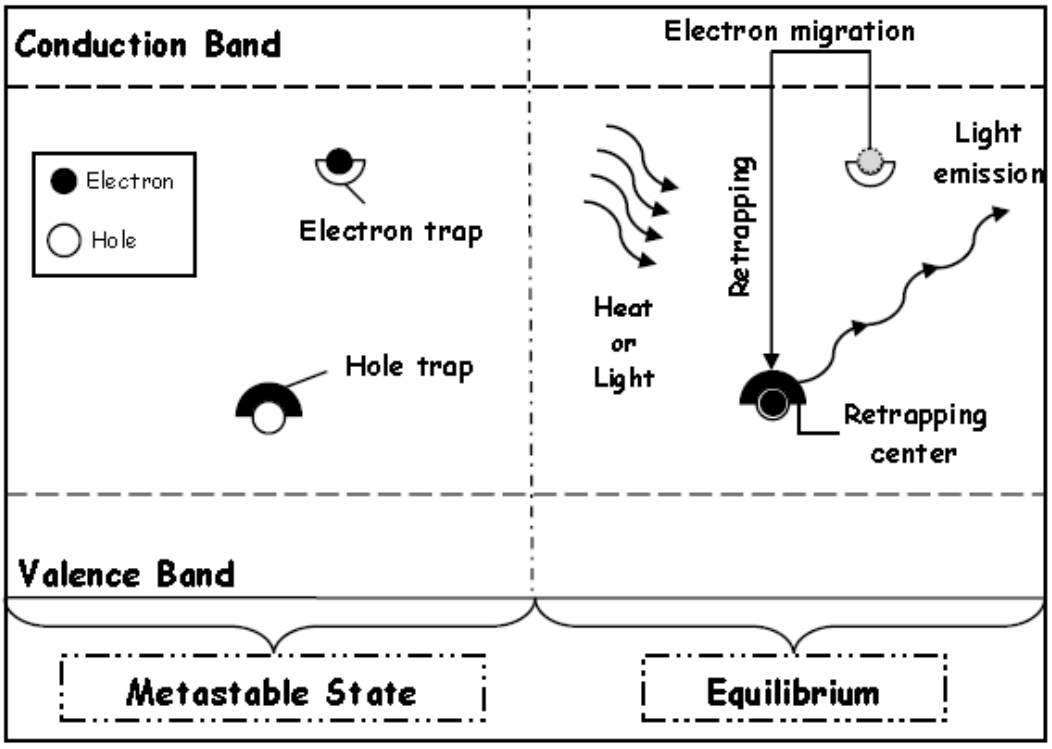

Figure 2.2 Energy-level diagram of the energy release stage for thermoluminescence processes [10].

2.4 Glow Curve

After the energy release, the output of the emitted light as a function of temperature is called thermoluminescence glow curve. The shape of the glow curves is one or more peaks of emitted light and some of them may overlap. Magnitudes and looks of the glow curves may change depending on the spectral response of the light sensitive device, different filter usage between the sample and the detector and heating rate. In addition, when the sample is irradiated it has only one shot effect. A second thermoluminescence emission cannot be recorded by cooling and reheating it unless it is irradiated again.

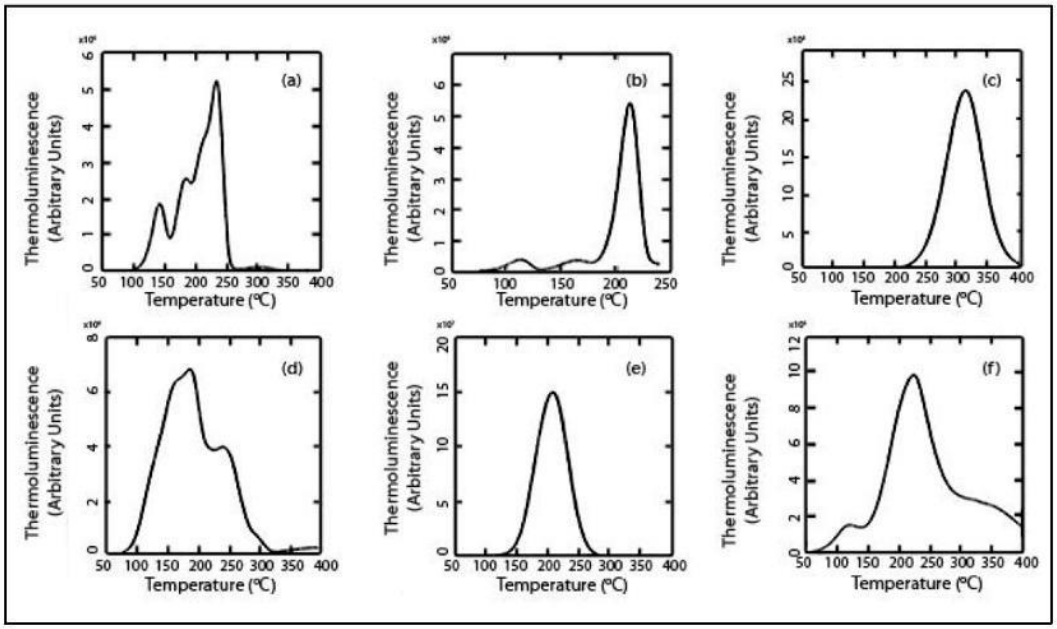

Figure 2.3 Glow curve examples of some thermoluminescent materials.

During a thermoluminescence experiment, one typically obtains several glow curves under different conditions. For example, a series of TL glow curves may be obtained for a material that was irradiated at several different doses, or was propelled at various temperatures. Usually the main goal of measuring and analyzing these TL glow curves is the extraction of several parameters that can be used to describe the TL process in the material. Examples of these the activation energy E for the TL traps (also called the trap depth), the frequency factors, the order of kinetics b of the TL process, the capture cross-sections for the traps and recombination centers, and the concentrations of these traps and centers.

2.5 Simple Thermoluminescence Model

The process by which materials emit light when heated can be understood by considering the simplest possible model consisting of two localized levels, an isolated electron trap (T) and a recombination center (RC), as shown in Figure 2.4. This is commonly referred to as the one-trap-one-recombination center model (OTOR).

Let us denote by N the total concentration of the traps in the crystal (m^{-3}), by n (t) the concentration of filled traps in the crystal (inm^{-3}). At time t, and by n_h(t)

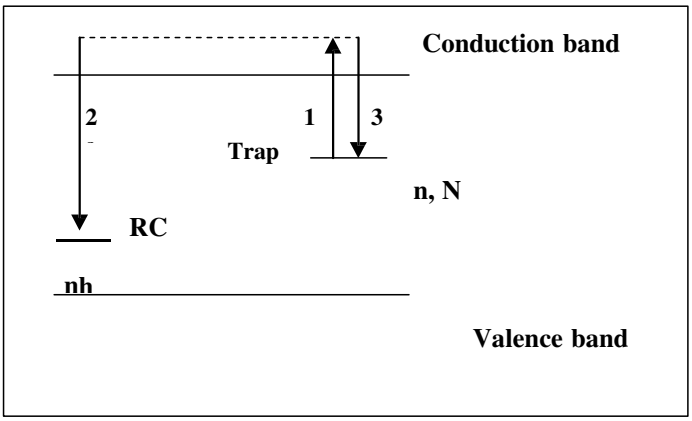

Figure 2.4. The simple two-level model for the thermoluminescence process [12]

2.5.1 First Order Kinetics

In 1945, Randall and Wilkins[13] extensively used a mathematical representation for each peak in a glow curve, starting from studies on the phosphorescence. Their mathematical treatment was based on the energy band model and yields the well-known first order expression. The following figure, Fig. 2.5, shows the simple model used for theoretical treatment. Between the delocalized bands, conduction band, CB, and valance band, VB, two localized levels (metastable states) are considered, one acting as a trap,*T*, and the other acting as a recombination center, *R*. The distance between the trap *T* and the bottom of the CB is called the activation energy or trap depth, *E*. This energy is the energy required to liberate a charge, i.e. , an electron, which is trapped in *T* [9].

The absorption of radiant energy with $h\gamma > E_g$ results in ionisation of valence electrons, producing energetic electrons and holes which will, after thermalization, produce free electrons in the conduction band and free holes in the valence band (transition a). The free charge carriers recombine with each other or become trapped. In the case of direct recombination an amount of energy will be released which may excite a luminescent centre. The luminescent centre relaxes (returns to the ground state) under the emission of light.
However, in semiconductors and insulators a certain percentage of the charge carriers is trapped: the electrons at T and the holes at R (transition b).

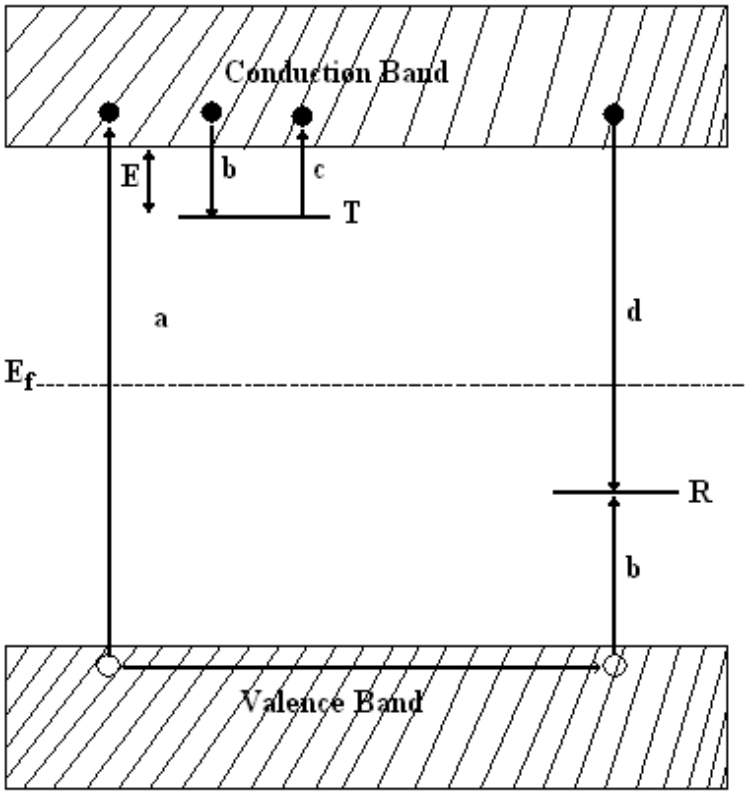

Figure 2.5. Energy band model showing the electronic transitions in a TL material according to a simple two-level model (a) generation of electrons and holes; (b) electron and hole trapping; (c) electron release due to thermal stimulation; (d) recombination. (●) shows electrons, (◦) shows holes. Level T is an electron trap, level R is a recombination centre, E_f is Fermi level[9]

The probability, *p*, per unit of time, that a trapped electron will escape from a trap, or the probability rate of escape per second, is given by the Arhenius equation, having considered that the electron in the trap have a Maxwellian distribution of thermal energies

$$p = s \exp\left\{-\frac{E}{kT}\right\} \qquad (2.1)$$

where *p* is the probability per unit time, *s* is the frequency factor, *k* the Boltzmann's constant, *E* is called the trap depth (eV) or activation energy, the energy needed to release an electron from the trap into the conduction band, *T* the absolute temperature (*K*) [2].

The intensity of TL $I(t)$ in photons per second at any time t during heating is proportional to the rate of recombination of holes and electrons at R. If m (m^{-3}) is the concentration of holes trapped at R the TL intensity can be written as

$$I(t) = -\frac{dm}{dt} \tag{2.2}$$

Here we assume that each recombination produces a photon and that all produced photons are detected. The rate of recombination will be proportional to the concentration of free electrons in the conduction band n_c and the concentration of holes m,

$$I(t) = -\frac{dm}{dt} = n_c mA \tag{2.3a}$$

with the constant A the recombination probability expressed in units of volume per unit time which is assumed to be independent of the temperature.

The rate of change of the concentration of trapped electrons n is equal to the rate of thermal release minus the rate of retrapping,

$$-\frac{dn}{dt} = np - n_c(N-n)A_r \tag{2.3b}$$

with N the concentration of electron traps and A_r the probability of retrapping (m^3/s). Likewise the rate concentration of free electrons is equal to the rate of thermal release minus the rate of retrapping and the rate of recombination,

$$\frac{dn_c}{dt} = np - n_c(N-n)A_r - n_c mA \tag{2.3c}$$

Equation (2.3a)-(2.3c) described the charge carrier traffic in the case of release of a trapped electron from a single-electron trap and recombination in a single centre. For TL produced by the release of holes the rate equations are similar to equation.(2.3a)-(2.3c). These equations form the basis of many analyses of TL phenomena. There is no general analytical solution. To develop an analytical expression some simplifying assumptions must be made. An important assumption is at any time

$$\left|\frac{dn_c}{dt}\right| << \left|\frac{dn}{dt}\right|, \qquad \left|\frac{dn_c}{dt}\right| << \left|\frac{dm}{dt}\right| \tag{2.4}$$

This assumption is called by Chen and McKeever [2] the quasi equilibrium assumption since it requires that the free electron concentration in the conduction band is quasistationary. The trapped electrons and holes are produced in pairs during the irradiation. Charge neutrality dictates therefore

$$n_c + n = m \tag{2.5}$$

which for $n_c \approx 0$ means that $n \approx m$ and

$$I(t) = -\frac{dm}{dt} \approx -\frac{dn}{dt} \tag{2.6}$$

Since $dn_c/dt \approx 0$ one gets from (2.3a) and (2.3b):

$$I(t) = \frac{mAns \exp\left\{-\frac{E}{kT}\right\}}{(N-n)A_r + mA} \tag{2.7}$$

Even (2.7) cannot be solved analytically without additional simplifying assumptions. Randall and Wilkins [13] assumed negligible retrapping during the heating stage, i.e. they assumed $mA >> (N-n)A_r$. Under this assumption equation (2.7) can be written

$$I(t) = -\frac{dn}{dt} = sn \exp\left\{-\frac{E}{kT}\right\} \tag{2.8}$$

This differential equation describes the charge transport in the lattice as a first-order process and the glow peaks calculated from this equation are called first-order glow peaks. Solving the differential equation (2.8) yields

$$I(t) = -\frac{dn}{dt} = n_o s \exp\left\{-\frac{E}{kT}\right\} \exp\left\{-s\int_0^t \exp\left\{-\frac{E}{kT(t')}\right\} dt'\right\} \tag{2.9}$$

where n_0 is the total number of trapped electrons at time t=0. Usually the temperature is raised as a linear function of time according to

$$T(t) = T_o + \beta t \tag{2.10}$$

with β the constant heating rate and T_0 the temperature at t=0. This gives for the intensity as function of temperature

$$I(T) = -\frac{1}{\beta}\frac{dn}{dt} = n_o \frac{s}{\beta} \exp\left\{-\frac{E}{kT}\right\} \exp\left\{-\frac{s}{\beta}\int_{T_o}^{T} \exp\left\{-\frac{E}{kT'}\right\} dT'\right\} \tag{2.11}$$

This is the well-known Randall–Wilkins first-order expression of a single glow peak. The peak has a characteristic asymmetric shape being wider on the low temperature side than on the high temperature side. On the low temperature side, i.e. in the initial rise of the glow peak, the intensity is dominated by the first exponential (exp(-*E*/*kT*)). Thus, if *I* is plotted as function of 1/*T*, a straight line is expected in the initial rise temperature range, with the slope of -*E*/*k*, from which the activation energy *E* is readily found.

The properties of the Randall–Wilkins equation are illustrated in Fig.2.6. In Fig.2.6(a) it is shown how $I(T)$ varies if n_0 varies from n_0=0.25 m^{-3} till n_0=2 m^{-3} while E=1 eV, s=1.0×10^{12} s^{-1} and β=1 K/s are kept constant.

It can be noted that the temperature at the peak maximum, T_m, stays fixed. This is a characteristic of all first-order TL curves. The condition for the maximum can be found by setting dI/dt=0 (or, somewhat easier from dln$I(T)$/dt=0). From this condition one gets;

$$\frac{\beta E}{kT_m^2} = s \exp\left\{-\frac{E}{kT_m}\right\} \tag{2.12}$$

In this equation n_0 does not appear which shows that T_m does not depend on n_0. From Fig .2.6 (a) it can be further seen that not only the peak height at the maximum but each point of the curve is proportional to n_0. In the application in dosimetry n_0 is the parameter of paramount importance since this parameter is proportional to the absorbed dose. It is simple to see that the area under the glow peak is equal to n_0 since

$$\int_0^\infty I(t)dt = -\int_0^\infty \frac{dn}{dt}dt = -\int_{n_0}^{n_\infty} dn = n_0 - n_\infty \tag{2.13}$$

and n_∞ is zero for $t\to\infty$. In Fig. 2.6 (b) the activation energy E has been varied from 0.8 to 1.2 eV. As E increases the peak shifts to higher temperatures with a decrease in the height and an increase in the width keeping the area (i.e. n_0) constant.

Similar changes can be noticed as s is varied (see Fig.2.6(c)) but now in the opposite way: as s increases the peak shifts to lower temperatures with an increase of the height and a decrease in width. In Fig. 2.6 (d) the heating rate has been varied. As β increases the peak shifts to higher temperatures while the height decreases and the width increases just as in the case of decreasing s. This can be expected since s and β appear as a ratio s/β in equation (2.11). It is worthwhile to note that of the four

parameters the activation energy E and the frequency factor s are the main physical parameters. They are called the trapping parameters and are fixed by the properties of the trapping centre. The other two parameters can be chosen by the experimenter by choosing a certain dose (n_0) and by read-out of the signal at a certain heating rate β. Investigation of a new TL material will therefore start with studying the glow peak behaviour under variation of the absorbed dose and the heating rate.

The evaluation of equation.(2.11) is hampered by the fact that the integral on the right-hand side is not elementary in the case of linear heating. Chen [14] has shown how the integral can be approximated by asymptotic series. In practical applications it is convenient to describe the glow peak in terms of parameters which are easy to derive experimentally, namely the intensity of peak at the maximum I_m and the temperature at the maximum T_m. Kitis et al. [15] have shown that equation (2.11) can be quite accurately approximated by

$$I(T) = I_m \exp\left[1 + \frac{E}{kT}\frac{T-T_m}{T_m} - \frac{T^2}{T_m^2}\exp\left\{\frac{E}{kT}\frac{T-T_m}{T_m}\right\}(1-\Delta) - \Delta_m\right] \qquad (2.14)$$

with $\Delta=2kT/E$ and $\Delta_m=2kT_m/E$. Recently Pagonis et al.[6] have shown that a Weibull distribution function also accurately describes the first-order TL curve. These expressions may be convenient for peak fitting purposes.

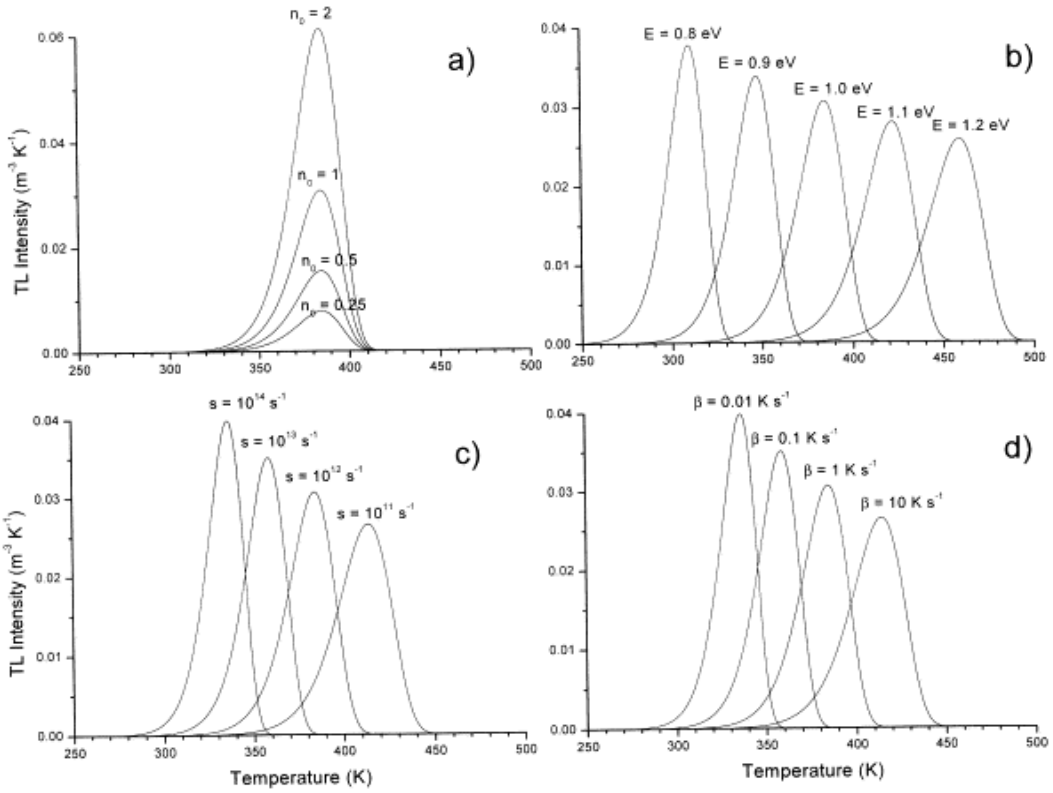

Figure 2.6. Properties of the R–W first-order TL equation, showing: (a) variation with n_0, the concentration of trapped charge carriers after irradiation; (b) the variation with E, the activation energy; (c) the variation with s, the escape frequency; (d) the variation with β, the heating rate. Parameter values: n_0=1 m^{-3}; E=1 eV; s=1×10^{12} s^{-1}, β=1 K/s of which one parameter is varied while the others are kept constant[2]

2.5.2 Second Order Kinetics

In 1948 Garlick and Gibson [16], in their studies on phosphorescence, considered the case when a free charge carrier has probability of either being trapped or recombining within a recombination center. The term second order kinetics is used to describe a situation in which retrapping is present i.e. i.e. $mA<<(N-n)A_r$

They assumed that the escaping electron from the trap has equal probability of either being retrapped or of recombining with hole ina recombination centre. Further they assume that the trap is far from saturation, i.e. $N>>n$ and $n=m$. With these assumptions, equation (2.7) becomes

$$I(t) = -\frac{dn}{dt} = s\frac{A}{NA_r}n^2 \exp\left\{-\frac{E}{kT}\right\} \tag{2.15}$$

We see that now dn/dt is proportional to n^2 which means a second-order reaction. With the additional assumption of equal probabilities of recombination and retrapping, A=A_r, integration of equation (2.15) gives

$$I(T) = \frac{n_0^2}{N}\frac{s}{\beta}\exp\left\{-\frac{E}{kT}\right\}\left[1+\frac{n_0 s}{N\beta}\int_{T_0}^{T}\exp\left\{-\frac{E}{kT'}\right\}dT'\right]^{-2} \tag{2.16}$$

This is the Garlick–Gibson TL equation for second-order kinetics. The main feature of this curve is that it is nearly symmetric, with the high temperature half of the curve slightly broader than the low temperature half. This can be understood from the consideration of the fact that in a second-order reaction significant concentrations of released electrons are re-trapped before they recombine, in this way giving rise to a delay in the luminescence emission and spreading out of the emission over a wider temperature range. The initial concentration n_0 appears here not merely as a multiplicative constant as in the first-order case, so that its variation at different dose levels change the shape of the whole curve. This is illustrated in Fig.2.3(a). It is seen that T_m decreases as n_0 increases. It can be derived [11] that the temperature shift can be approximated by

$$T_1 - T_2 \approx T_1 T_2 \frac{k}{E}\ln f \tag{2.17}$$

where T_1 is the temperature of maximum intensity at a certain dose and T_2 the temperature of maximum intensity at f times higher dose. With the parameter values of Fig.2.7(a) the shift is 25 K. When E=1 eV, T_1=400 K and the absorbed dose is increased by a factor 1000, which is easy to realise experimentally, a temperature shift of 77 K can be expected. From equation (2.17) it follows further that for a given increase of the dose the shallower the trap, i.e., the smaller E, the larger the peak shift. Fig. 2.7(b) illustrates the variation in size and position of a second-order peak as function of E, in Fig.2.7(c) s function of s/N, and in Fig.2.7(d) as function of the heating rate. The area under the curve is, as in the case of first-order kinetics, proportional to the initial concentration n_0 but the peak height is no longer directly proportional to the peak area, although the deviation is small.

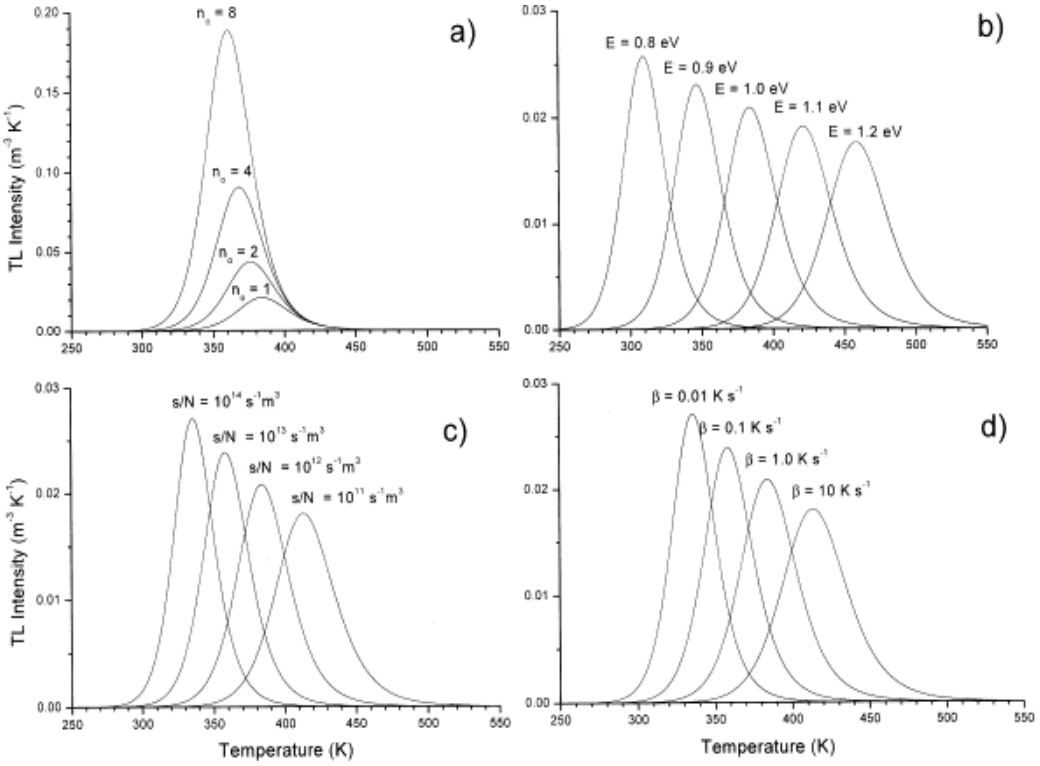

Figure 2.7. Properties of the Garlick–Gibson second-order TL equation, showing: (a) variation with n_0, the concentration of trapped charge carriers after irradiation; (b) the variation with E, the activation energy; (c) the variation with s/N; (d) the variation with β, the heating rate. Parameter values: n_0=1 m^{-3}; E=1 eV; s/N=1×10^{12} s^{-1} m^3, β=1 K/s of which one parameter is varied while the others are kept constant[2]

Note that, similarly to the first-order case, the term dominating the temperature dependence in the initial rise is exp(-E/kT). So the `initial rise method' for the determination of the trap depth can be applied here as well.

Also for second-order kinetics the glow peak shape, equation (2.16) can be approximated with a function written in terms of maximum peak intensity I_m and the maximum peak temperature T_m

$$I(T) = 4I_m \exp\left(\frac{E}{kT}\frac{T-T_m}{T_m}\right) \times \left[\frac{T^2}{T_m^2}(1-\Delta)\exp\left\{\frac{E}{kT}\frac{T-T_m}{T_m}\right\} + 1 + \Delta_m\right]^{-2} \qquad (2.18)$$

with Δ and Δ_m the same meaning as in equation (2.14).

2.5.3 General order kinetics

When the conditions of first or second order kinetics are not satisfied, one obtains the so called general order kinetics which deals with intermediate cases. May and Partridge (1964) [17] wrote an empirical expression for taking into account experimental situations which indicated intermediate kinetic process. They started with the assumption that the energy level of traps is single, as already assumed for the first and second orders.

For general – order kinetics

$$I(t) = -\frac{dn}{dt} = n^b s' \exp\left\{-\frac{E}{kT}\right\} \tag{2.19}$$

where s' has the dimension of $m^{3(b\text{-}1)}$ s^{-1} and b is defined as the general-order parameter and is not necessarily 1 or 2. Integration of equation (2.19) for $b \neq 1$ yields

$$I(T) = \frac{s''}{\beta} n_0 \exp\left\{-\frac{E}{kT}\right\}\left[1 + (b-1)\frac{s''}{\beta}\int_{T_0}^{T} \exp\left\{-\frac{E}{kT'}\right\} dT'\right]^{-b/(b-1)} \tag{2.20}$$

where now $s''=s' n_0^{b\text{-}1}$ with unit s^{-1}. Equation (2.20) includes the second-order case (b=2) and reduces to equation (2.11) when $b \to 1$. It should be noted that according to equation (2.19) the dimension of s' should be $m^{3(b\text{-}1)}$ s^{-1} that means that the dimension changes with the order b which makes it difficult to interpret physically. Still, the general-order case is useful since intermediate cases can be dealt with and it smoothly goes to first- and second-orders when $b \to 1$ and $b \to 2$, respectively (see Fig.2.4).

Methods of Analysis 2.6

Since the pioneering work of Randall & Wilkins and Garlick & Gibson there has been a plethora of published papers dealing with methods by which the trapping parameters (mainly E and s) can be obtained from a glow-curve. Some utilize simple formulae; others consist of elaborate curve- fitting procedures. The determination of trapping parameters from thermoluminescence glow curves has been a subject of interest for half a century. There are various methods for evaluating the trapping parameters from the glow curves [9-10,]. When one glow peak is highly isolated from the others, the experimental methods such as initial rise, variable heating rates,

isothermally decay, and peak shape methods are suitable methods to determine these parameters.

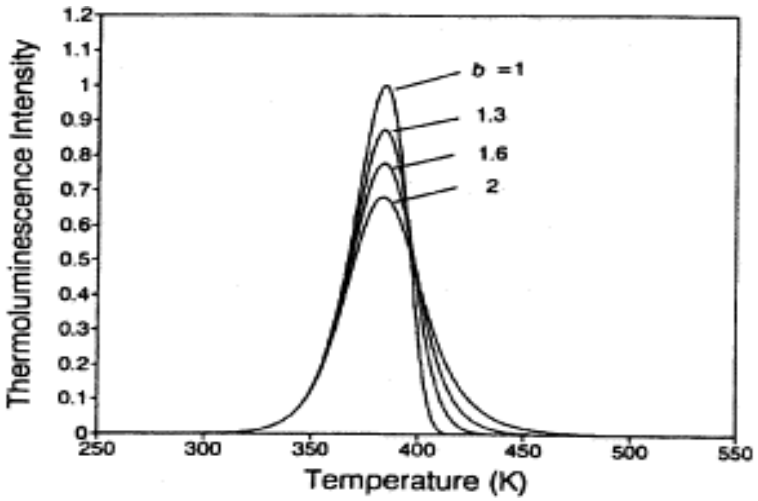

Figure 2.8. Comparison of first-order (b=1), second-order (b=2) and intermediate-order (b=1.3 and 1.6) TL peaks, with E=1 eV, s=1×10^{12} s^{-1}, n_0=N=1 m^{-3} and β=1 K/s (from [12]).

2.6.1 Initial Rise Method

This method stems from the recognition by Garlick&Gibson (1948) that the initial rise part of a thermoluminescence curve is exponentially dependent on temperature according to

$$I(T) = C\exp(-E/kT) \tag{2.21}$$

where the constant C includes all the dependencies on the other parameters and occupancies, E is the activation energy (eV), k is the Boltzmann`s constant (eV/K^{-1}) and T is the temperature (K)[18-19]

Plotting ln(I) against $1/T$ a linear plot is obtained with slope equal to $-E/k$. Hence it is possible to evaluate E without any knowledge of the frequency factor s by means of equation

$$E = -kd(\ln(I))/d(1/T) \tag{2.22}$$

Once the value of E was determined, the frequency factor (s) was obtained from the equation

$$\frac{\beta E}{kT_m} = s\exp(-\frac{E}{kT}) \tag{2.23}$$

where T_m is the temperature at the maximum intensity. This method can only be used when the glow peak is well defined and clearly separated from the other peaks [20-22].

2.6.2 Heating Rate Method

Another important method is various heating rates for the determination of activation energies. If a sample is heated at two different linear heating rates β_1 and β_2 the peak temperatures will be different. Equation (2.23) can therefore, be written for each heating rate and dividing the equation for β_1 (and T_{m1}) by the equation for β_2 (and T_{m2}) and rearranging, one gets an explicit equation for the calculation of E [23-25]

$$E = k\frac{T_{m1}T_{m2}}{T_{m1} - T_{m2}}\ln[(\frac{\beta_1}{\beta_2})(\frac{T_{m2}}{T_{m1}})^2] \tag{2.24}$$

The major advantage of the heating rate method is that it only requires data to be taken at a peak maximum (T_m, I_m) which, in case of a large peak surrounded by smaller satellites, can be reasonably accurately determined from the glow curve. Furthermore the calculation of E is not affected by problems due to thermal quenching, as with the initial rise method [26].

When various heating rates for the first-order kinetics are used, the following expression is obtained:

$$\ln(\frac{T_m^{\ 2}}{\beta}) = (\frac{E}{k})(\frac{1}{Tm}) + cons\tan t \tag{2.25}$$

A plot of ln (T_m^2/β)versus ($1/ T_m$) should yield a straight line with a slope E/k, then E is found. Additionally, extrapolating to $1/T_m = 0$, a value for $ln(sk/E)$ is obtained from which s can be calculated by inserting the value of E/k found from the slope [27]. This method of various heating rates are applicable for general-order kinetics which includes the second-order case. For the general order case, one can plot

$ln\left[I_m^{\ b-1}(T_m^{\ 2}/\beta)^b\right]$ versus $1/T_m$, whose slope is equal to E/k.

2.6.3 Peak Shape Method

In contrast to partial or whole peak analysis, methods based on the shape of the peak utilize just two or three points from the glow-curve. Usually, these are the maximum of the peak T_m and either, or both, the low-and high-temperature half height at T_1 and T_2. Evaluation of E from the shape of the peak utilising parameters such as T_m, full width at half-maximum $\omega=T_2-T_1$, half width on the high temperature side of the maximum $\delta=T_2-T_m$, half width on the low-temperature side of the maximum $\tau=T_m-T_1$, and $\mu_g=\delta/\omega$ called the shape parameter [28].

The order of kinetics b can be estimated by means of shape parameters. Chen [29] found that μ_g is not sensitive to changes in E and s, but it changes with the order of kinetics b. It has been shown that the ranges of μ_g varies from 0.42 for b=1 to 0.52 for b=2 in case of linear heating. The first peak shape method was developed by Grossweiner [30]; later Chen [31] modified Halperin and Braner's equations [32] for calculating E values;

$$
\begin{aligned}
E_\tau &= \left[1.51+3(\mu_g-0.42)\right]\frac{kT_m^2}{\tau}-\left[1.58+4.2(\mu_g-0.42)\right]2kT_m \\
E_\delta &= \left[0.976+7.3(\mu_g-0.42)\right]\frac{kT_m^2}{\delta} \\
E_\omega &= \left[2.52+10.2(\mu_g-0.42)\right]\frac{kT_m^2}{\omega}-2kT_m
\end{aligned}
\tag{2.26}
$$

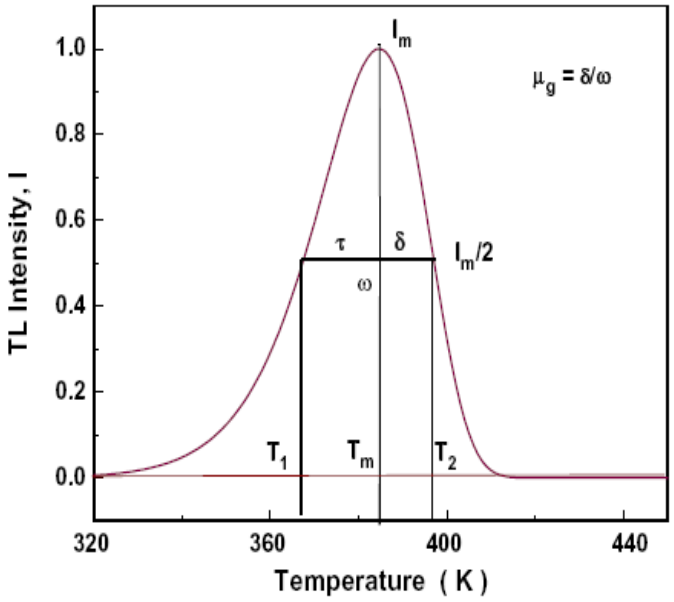

Figure 2.9 The characteristics points on a TL glow-peak, which define the peak-shape parameters[12].

After determination of the activation energy and the order of kinetics, using the following expressions the frequency factor *s*, it must be noted that this parameter called as pre-exponential factor in the general order kinetic, can be estimated for first and general order kinetics respectively.

$$s = \frac{\beta E}{kT_m^2} \exp\left[\frac{E}{kT_m}\right]$$
$$s = \frac{\beta E}{kT_m^2}\left[\exp(-\frac{E}{kT_m})(1+(b-1)\frac{2kT_m}{E})\right]^{\frac{b}{b-1}} \qquad (2.27)$$

2.6.4 Computerized Glow Curve Deconvolution

Instead of employing simple formula to derive values for the parameters *E*, *s* and *b*, methods of computerized curve fitting have been used on several occasions with apparent success. The procedure is to establish the approximate positions of the most prominent peaks in the glow-curve and to estimate initial values of *E*, *s,* and *b* by using one of the analytical methods discussed so far. A theoretical curve is then computed using the general-order equation for $b \neq 1$, or the first-order equation for $b=1$. The computed curve is then compared with the actual experimental curve and a root mean square (RMS) deviation between the two is calculated. The procedure continues by sequentially changing the *E*, *s*, and *b* values until a minimum value of the RMS deviation is obtained. This method has the advantage over experimental methods in that they can be used in largely overlapping-peak glow curves without resorting to heat treatment [6].

The program was developed at the Reactor Institute at Delft, The Netherlands [32]. This program is capable of simultaneous deconvolutionas many as nine glow peaks from glow curve. Two different models were used in the computer program. In the first model, the glow curve is approximated from first order TL kinetic by the expression,

$$I(T) = n_0 s \exp(-\frac{E}{kT})\exp\left[(-\frac{s}{\beta}\frac{kT^2}{E}\exp(-\frac{E}{kT}) * (0.9920 - 1.620\frac{kT}{E_a})\right] \qquad (2.28)$$

In the second model the glow curve is approximated with general order TL kinetics by using the expression,

$$I(T) = n_0 s \quad \exp(-\frac{E}{kT})\left[1+(-\frac{(b-1)s}{\beta}\frac{kT^2}{E}\exp(-\frac{E}{kT})*(0.9920-1.620\frac{kT}{E_a})\right]^{\frac{b}{b-1}} \quad (2.29)$$

where n_0 (m^{-3}) is the concentration of trapped electrons at t=0, s (s^{-1}) is the frequency factor for first-order and the pre-exponential factor for the general-order, E (eV) the activation energy, T (K) the absolute temperature, k (eVK^{-1}) Boltzmann's constant, β ($^0Cs^{-1}$) heating rate and b the kinetic order.

The summation of overall peaks and background contribution can lead to composite glow curve formula as shown below

$$I(T) = \sum_{i=1}^{n} I_i(T) + a + b\exp(T) \quad (2.30)$$

where $I(T)$ is the fitted total glow curve, a allows for the electronic noise contribution to the planchet and dosimeters infrared contribution to the background.

Starting from the above equation (2.30), the least square minimisation procedure and also FOM (Figure of Merit) was used to judge the fitting results as to whether they are good or not. i.e.

$$FOM = \sum_{i=1}^{n}\frac{|N_i(T)-I(T)|}{A} = \sum_{i=1}^{n}\frac{|\Delta N_i|}{A} \quad (2.31)$$

where $N_i(T)$ is the i-th experimental points (total n=200 data points), $I(T)$ is the i-th fitted points, and A is the integrated area of the fitted glow curve.

From many experiences [37-38], it can be said that if the values of the FOM are between 0.0% and 2.5% the fit is good, 2.5 % and 3.5% the fit is fair, and > 3.5% it is bad fit.

To have a graphic representation of the agreement between the experimental and fitted glow curves, the computer program also plots the function,

$$X(T) = \frac{N_i(T)-I_i(T)}{\sqrt{I_i(T)}} \quad (2.32)$$

which is a normal variable with an expected value 0 and σ=1 where $\sigma^2(T)=I_i(T)$.

CHAPTER 3

TL DOSE RESPONSE MODELS

3.1 Overview

In this chapter, we have described several examples of modular theory, which describes the thermoluminescence in a variety of materials and so presence of great significance in scientific applications of the subject. As well as dosimetry and radiation protection that transmits the signal TL to a dose of articles based on thermoluminescence. And also we will describe several of the terms used to describe the nonlinear material. The first section of this chapter gives an overview of nonlinear response exhibited by several materials, and introduces the terminology used in describing these nonlinearities. In the second section I will explain the competition between traps and then describe how to be during irradiation so that they can be on the basis of the presence of a considerable number of models forms of kinetic models. The third section i will describes a more complex case in which competition phenomena are of importance during both the excitation and the heating stage of TL. The fourth section i will provides an example of obtaining the superlinearity index g(D) and the superlinearity index f (D) from experimental TL versus dose curves. The quantities f(D) and g(D) are defined in the next section.

3.2. Nonlinear Dose Response of TL Materials and Terminology

In this section we will gives some fundamental concepts and terminology is presented, relevant to experimentally observed nonlinear dose response of TL materials to radiation. Several important TL materials exhibit a nonlinear dose response that can be expressed in the mathematical form:

$$I_{\max} = \alpha D^{k} \tag{3.1}$$

Where I_{max} represents the maximum TL intensity (or the TL integral D is the dose of the radiation). a and k are constants.

When I_{max} is plotted as a function of the dose D on a log–log scale, this equation yields a straight line with a slope k that may be larger than unity. For example, Halperin and Chen [15] found that the dose response of UV (ultra violet) irradiated diamonds exhibited a slope k between 2 and 3 at certain wavelengths. These authors suggested the term superlinearity to describe this more than linear dose response. Chen and McKeever [44] suggested using the term superlinearity for the increase of the derivative of the dose of the TL response function. If the measured TL signal is S(D), the increase in the derivative of S(D) is expressed by the fact that the second derivative $d^2 S/dD^2 > 0$. Cases where $d^2S/dD^2 < 0$ are characterized as sublinear, and cases where $d^2S/dD^2 = 0$ are characterized as a linear dose response. These authors defined the following dimensionless quantity termed the superlinearity index g(D):

$$g(D) = [\frac{DS''(D)}{S'(D)}] + 1 \tag{3.2}$$

As long as $S'(D) > 0$, a value of $g(D) > 1$ signifies superlinearity, while a value of $g(D) = 1$ denotes a linear dose response, and $g(D) < 1$ signifies sublinearity. In the special case where $S(D) = \alpha D^k + \beta$, one obtains $g(D) = k$. The application of equation (3.2) requires the knowledge of an analytical expression which can fit the experimentally obtained TL dose response curves. Otherwise, this equation cannot be applied to the experimental data. In some low dose ranges several TL materials show linear dose dependence, followed by a superlinear dose range and by a sublinear range while approaching saturation. Chen and McKeever suggested using the term superlinearity to describe this particular nonlinear dose response. Some authors [45] quantified this behavior by introducing the following dimensionless function termed the superlinearity index or dose response function f (D):

$$f(D) = [\frac{S(D)/D}{S(D_1)/D_1}] \tag{3.3}$$

Where D_1 is a normalization dose in the initial linear range. Values of $f(D) > 1$ indicate values of S(D) above the initial linear range. In summary, superlinearity is

a measure of the rate of change of the dose response with the dose, and is described quantitatively by the superlinearity index g(D). On the other hand, superlinearity is described quantitatively by the superlinearity index f (D), and is mostly used in TL applications in dating and dosimetry. Rodine and Land [46] suggested that the superlinear behavior of some materials might be explained by competition during the heating phase, instead of competition during the excitation stage. Within the framework of such models, the initial dose dependence of the TL response may be quadratic in nature. Kristiapoller et al [39] developed a mathematical formulation of TL models of this type. Chen and Fogel [47] discussed some of the disadvantages of these two separate approaches, especially the main assumption that when competition occurs during the irradiation stage, no competition takes place during the heating phase, and vice versa. These authors developed a model that combines the characteristics of the two models: competition during heating and competition during excitation models.

3.3 The Filling of Traps in Crystals during Irradiation

The model consists of one trapping state and one recombination center during irradiation is shown in Figure 3.1. The figure indicates the allowed electron and hole transitions from the conduction and the valence band. The trap is characterized by total concentration N in the crystal and by instantaneous electron occupancy n(t). The recombination center has instantaneous hole occupancy $n_h(t)$ and total concentration N_h in the crystal. The functions $n_c(t)$ and $n_v(t)$ represent the instantaneous concentrations of free electrons in the conduction band and free holes in the valence band correspondingly. The equations describing the rate of change of the functions n(t), $n_h(t)$, $n_c(t)$, and $n_v(t)$ during the irradiation process are [45].

$$\frac{dn}{dt} = n_c(N-n)A \tag{3.4}$$

The equation (3.4) describes mathematically the fact that electrons in the conduction band can be trapped into the electron trap.

$$\frac{dn_c}{dt} = R - n_v(N_h - n_h)A_h \tag{3.5}$$

The equation (3.5) describes the process by which free holes in the valence band are created at a constant rate R during the excitation, and these holes can also be trapped from the valence band into the recombination center as indicated by the term $-n_v(N_h - n_h)\, A_h$.

$$\frac{dn_c}{dt} = n_v\left(N_h - n_h\right)A_h - n_c - n_h A_r \tag{3.6}$$

The Eg (3.6) describes the fact that the concentration of holes in the recombination center is changed by either trapping electrons from the conduction band (term-$n_c n_h A_r$), or by trapping holes from the valence band (term $n_v(N_h - n_h)\, A_h$).

$$\frac{dn_c}{dt} + \frac{dn}{dt} = \frac{dn_h}{dt} + \frac{dn_v}{dt} \tag{3.7}$$

The Eg (3.7) describes the conservation of total charge in the crystal, with the left-hand side being equal to the total instantaneous concentration of electrons, and the right- hand side representing the total concentration of holes in the crystal at any time t. The parameters in the above expressions are as follows:

A = transition probability coefficient of electrons into the trap ($cm^3\ s^{-1}$).

A_h = trapping probability coefficient of holes from the valence band into the recombination center ($cm^3\ s^{-1}$).

A_r = recombination probability coefficient of electrons from the conduction band into the recombination center ($cm^3\ s^{-1}$).

n = instantaneous concentration of electrons in the electron trap at time t (cm^{-3}).

N = total concentration of electron traps in the crystal (cm^{-3}).

(N − n) = instantaneous concentration of empty main traps available at time t.

n_h = instantaneous concentration of holes in the recombination center(cm^{-3}).

N_h = total concentration of holes in the crystal (cm^{-3}).

n_c = instantaneous concentration of electrons in the conduction band (cm^{-3}).

n_v = instantaneous concentration of holes in the valence band (cm^{-3}).

R = constant rate of production of electron–hole pairs per cm^3 per second $(cm^{-3} s^{-1})$.

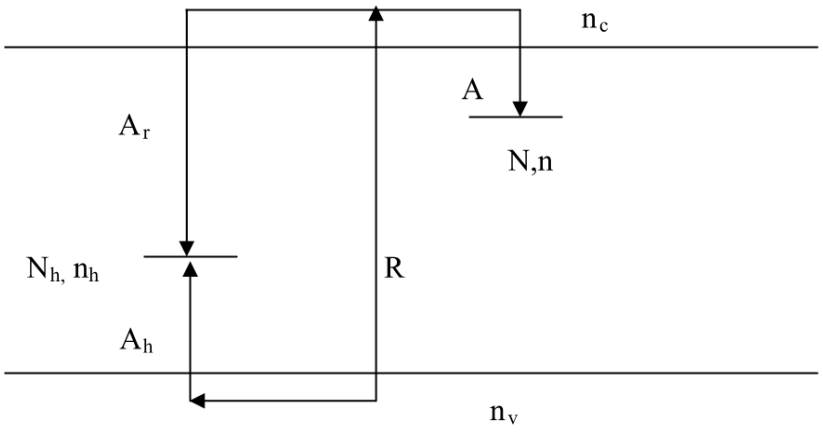

Figure 3.1 Kinetic model for the filling of traps during crystal irradiation [6]

3.4 Competition during Excitation Model

This model can be expressed by using the figure 3.2. The model has two electrons trapping states and is characterized by the total concentrations of these electrons N_1 and N_2 and instantaneous occupancies $n_1(t)$ and $n_2(t)$, respectively [48]. The first trap is the one responsible for TL. trap as the second competitor trap The form also contains a recombination center and the instantaneous occupancy hole and when our audit process raised irradiation of electrons in the valence band in conduction band and be trapped either n_1 and n_2 or with a couple of traps that are competing for electrons as shown in Figure(3.2). The kinetic equations for this model are:

$$\frac{dn_1}{dt} = A_1(N_1 - n_1)n_c \tag{3.8}$$

$$\frac{dn_2}{dt} = A_2(N_2 - n_2)n_c \tag{3.9}$$

The equation (3.8) and (3.9) describes mathematically the fact that electrons in the conduction band can be trapped into either the main or into the competitor trap.

$$\frac{dn_c}{dt} = R - \frac{dn_1}{dt} - \frac{dn_2}{dt} - A_K n_c p \tag{3.10}$$

The equation (3.10) describes the fact that the electrons in the conduction band are produced by the constant excitation rate R, and can also be trapped into either of the two traps (terms $-\frac{dn_1}{dt}$ and $-\frac{dn_2}{dt}$) or into the recombination center (term $-A_k n_c p$).

$$p = n_1 + n_2 + n_c \tag{3.11}$$

The equation (3.11) describes the conservation of total charge in the crystal, with the left-hand side being equal to the concentration of holes trapped in the recombination center, and the right-hand side representing the total concentration of electrons in the crystal at any moment t. the Eg (3.11)is based on the assumption that the concentration of free holes in the valence band can be neglected as compared with the accumulated concentration of holes p(t).

The parameters in the above expressions are as follows:

A_1 = transition probability coefficient of electrons into the main trap ($m^3\ s^{-1}$).

A_2 = transition probability coefficient of electrons into the competitor trap ($m^3\ s^{-1}$).

A_k = transition probability coefficient of electrons from the conduction band into the recombination center ($m^3\ s^{-1}$).

n_1 = instantaneous concentration of electrons in the main trap at time t (m^{-3}).

N_1 = total concentration of main traps in the crystal (m^{-3}).

$(N_1 - n_1)$ = instantaneous concentration of empty main traps available at time t.

n_2 = instantaneous concentration of electrons in the competitor trap (m^{-3}).

N_2 = total concentration of competitor traps in the crystal (m^{-3}).

n_c = instantaneous concentration of electrons in the conduction band (m^{-3})

R = constant rate of production of electron–hole pairs per m^3 per second ($m^{-3}s^{-1}$)

p = instantaneous concentration of holes in the recombination center (m^{-3})

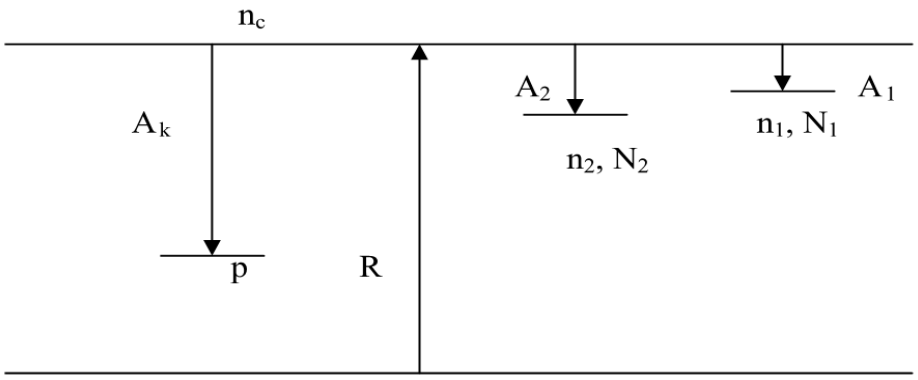

Figure 3.2 the competition during excitation model [12]

3.5 Superlinearity Model with Competition during Both Excitation and Heating

The figures 3.3 and 3.4 show the superlinearity model with competition during both excitation and heating [49]. The form is a two trapping states and is characterized by the total concentrations of these electrons N_1 and N_2 and instantaneous occupancies $n_1(t)$ and $n_2(t)$, respectively. The first trap is the one responsible for TL. trap as the second competitor trap The form also contains a recombination center and the instantaneous occupancy hole and total concentration of hole traps given by M.

It is expressed in three stages the irradiation process, an intermediate relaxation stage, and the heating (measurement of TL) stage. When our audit process raised irradiation of electrons in the valence band in conduction band and be trapped both n_1 and n_2 or with a couple of traps that are competing for electrons. These electrons in the conduction band May combine with holes in the recombination center at the same time. In the irradiation process an equal number of holes are created in the valence band. And these holes can be trapped directly into the recombination center increasing the hole occupancy m(t).

The kinetic equations for the excitation stage in this model are:

$$\frac{dn_1}{dt} = A_1(N_1 - n_1)n_c \tag{3.12}$$

$$\frac{dn_2}{dt} = A_2\left(N_2 - n_2\right)n_c \tag{3.13}$$

The Equations (3.12) and (3.13) describes mathematically the fact that electrons in the conduction band can be trapped into either the main or the competitor trap.

$$\frac{dn_m}{dt} = A_n n_v\left(M - m\right)A_m m n_c \tag{3.14}$$

The Eg (2.14) describes the fact that the number of holes in the recombination center is changed by either trapping additional holes from the valence band (term-$A_n n_v(M-m)$), or by trapping electrons from the conduction band (term $-A_m m n_c$).

$$\frac{dn_v}{dt} = R - A_n n_v\left(M - m\right) \tag{3.15}$$

The Eg (3.15) describes the fact that holes are produced continuously in the valence band by the excitation rate R, but they are also captured into the recombination center (term $-\ A_n n_v(M - m)$).

$$\frac{dn_c}{dt} + \frac{dn_1}{dt} + \frac{dn_2}{dt} = \frac{dm}{dt} + \frac{dn_c}{dt} \tag{3.16}$$

The Eg (3.16) describes the conservation of total charge in the crystal, with the left-hand side being equal to the total rate of change of the concentration of holes, and the right-hand side being equal to the total rate of change of the concentration of electrons in the crystal.

The parameters in the above expressions are as follows:

A_1 = transition probability coefficient of electrons into the main trap ($m^3\ s^{-1}$).

A_2 = transition probability coefficient of electrons into the competitor trap ($m^3\ s^{-1}$).

A_m = transition probability coefficient of electrons from the conduction band into the recombination center ($m^3\ s^{-1}$).

A_n = capture probability coefficient of holes from the valence band into the recombination center ($m^3\ s^{-1}$).

n_1 = instantaneous concentration of electrons in the main trap at time t (m^{-3}).

N_1 = total concentration of main traps in the crystal (m^{-3}).

$(N_1 - n_1)$ = instantaneous concentration of empty main traps available at time t.

n_2 = instantaneous concentration of electrons in the competitor trap (m^{-3}).

N_2 = total concentration of competitor traps in the crystal (m^{-3}).

n_c = instantaneous concentration of electrons in the conduction band (m^{-3}).

n_v = instantaneous concentration of holes in the valence band (m^{-3}).

R = constant rate of production of electron–hole pairs per m^3 per second (m^{-3} s^{-1}).

m = instantaneous concentration of holes in the recombination center (m^{-3}).

M = total concentration of holes in the crystal (m^{-3}).

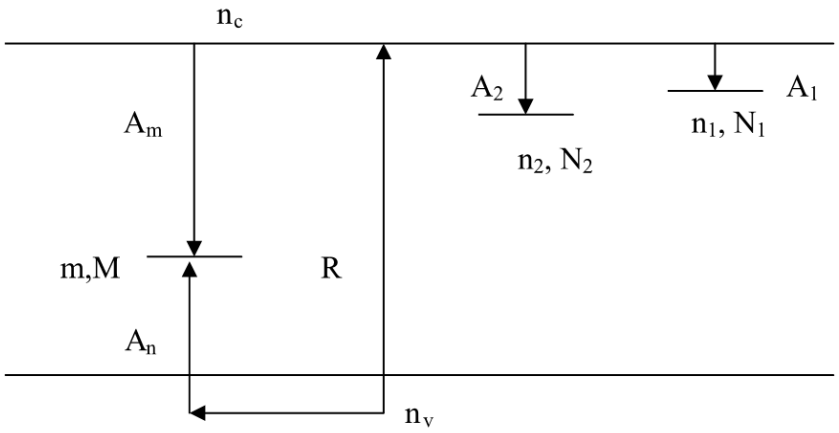

Figure 3.3 Model with competition during both excitation and heating: irradiation stage [12]

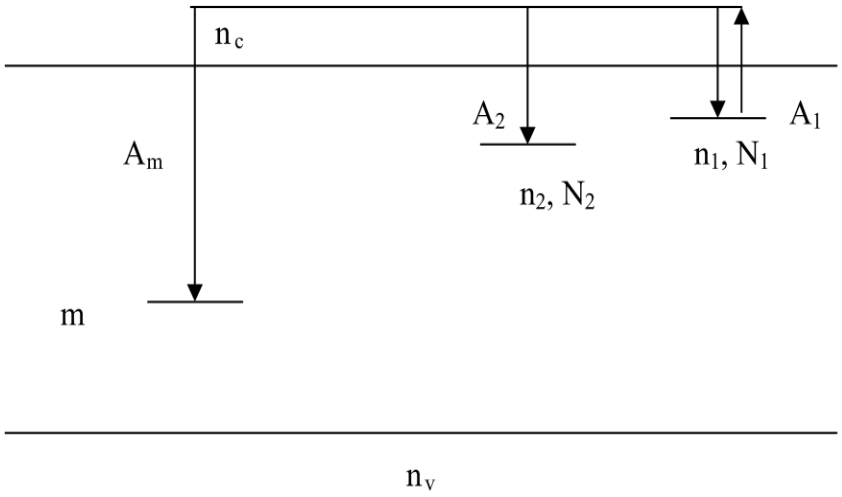

Figure 3.4 Model with competition during both excitation and heating: heating stage[12]

3.2.6 The f(D) Function

Figure 3.5 shows the plot y(D) versus D obtained from the data. The experimental data have been fitted by the following equation

$$y(D) = A(1 - \exp(-BD)) - cD\exp(-BD) \tag{3.17}$$

Where D is the given dose, A is the TL response at the saturation level (4844 a.u)**,**

B = 0.291 × 10^{-2} Gy^{-1}, and C = 12.93 Gy^{-1}.

The superlinearity index f (D) is used in the case where the main interest is in the amount of deviation from linearity, i.e., whether the TL signal is above or below the linear extrapolated range, and to make corrections if needed [50].

While the superlinearity index f (D) is defined as

$$f(D) = [\frac{S(D)/D}{S(D_1)/D_1}] \tag{3.18}$$

The following is the meaning of the symbols used in the two previous equations**:**

- y denotes the TL signal obtained at a given dose D.
- y = y(D) is the analytical expression giving the behavior of y as a function of dose D and it is found by fitting the experimental values.
- y′(D) and y′′(D) are, respectively, the first and second derivatives of the function y(D).
- D_1 is the normalization dose in the initial linear range of the y = y(D) curve

In a similar manner, f (D) < 1 means a sublinear region, f (D) ~ 0 means a saturation region and f (D) > 1 indicates a superlinearity region.

The general features concerning the TL versus dose behavior can be outlined as follows:

- if y′′ (D) > 0, y′(D) and y(D) increase with D and y(D) is supralinear,
- if y′′(D) < 0, y′(D) and y(D) decrease with D and y(D) is sublinear.
- if y′′(D) = 0, y′(D) is constant with D and y(D) is linear.

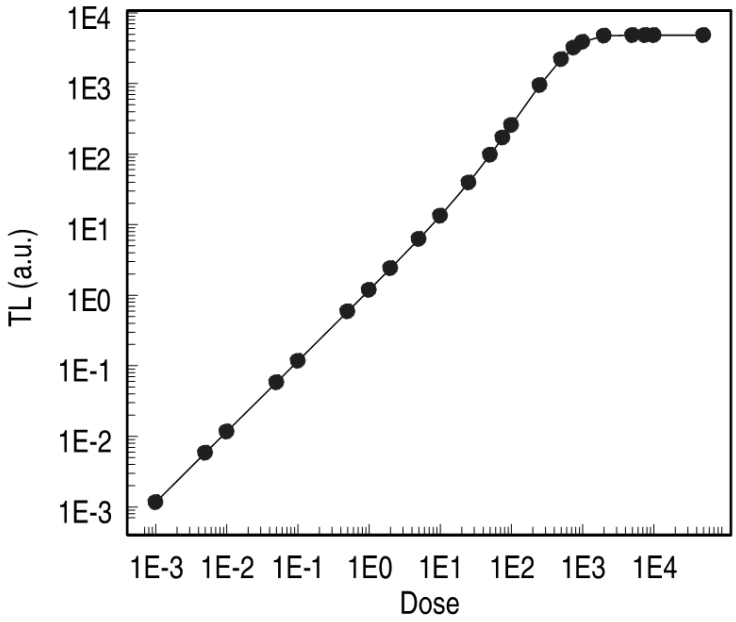

Figure 3.5 Plot of the TL response versus dose [12]

CHAPTER 4

EXPERIMENTAL PROCEDURE

The materials, equipments and experimental procedures were used in this work were described below.

4.1 Calcium sulphate (CaSO4: Dy)

The material that performed in this study was Calcium sulphate doped with dysprosium ($CaSO_4$:Dy) (TLD-900) from Thermo Electron Corporation. The dimensions of this sample are (1.8 x 1.8 x 0.35 mm^3), with a mean mass of (0.245g). Thermoluminescence dosimeters (TLD) like manganese. The method of preparation was first described by Yamashita [33] and later variants [34] produced highly sensitive material.

Calcium sulphate doped with dysprosium ($CaSO_4$: Dy) is a solid state material and in the past two decades has been taken in the investigation for detecting and measuring radiation. Solid state materials (principally $CaSO_4$:Dy) used as thermoluminescent dosimeters are synthesized mainly in the form of crystalline powder by the precipitation and crystallization method [35] other authors have used $CaSO_4$:Dy in pellet form mixed with Teflon (PTFE) [15]. Thermoluminescent response in $CaSO_4$:Dy is essentially affected by the synthesis preparation method, heat thermal treatment history, particle size [36] in the crystal structure, the type of precursors used, as well as the dopant concentration.

Other authors have centered their works on the thermoluminescent (TL) response in materials such as calcium sulphate doped with rare earths ($CaSO_4$:RE, eg. Dy, Eu,Tm) during the last forty years. These authors focused their purpose on the thermoluminescent properties to be considered as radiation detectors, including: fading of the TL response as a function of storage time, high sensitivity and stability in $CaSO_4$:Dy [37]. Other investigations are focused on dosimetric characteristics of $CaSO_4$:Dy for measuring different kinds of radiation e.g: X-rays,

beta rays, high energy electrons [38] and high doses of 60Co [39]. Nunes and Campos [40] observed $CaSO_4$:Dy sensitivity compared with LiF:Mg,Ti and they proposed they are good for use in the radiation therapy area using high energy electrons beams. With Z_{eff}=15.5, CaSO4 displays a significant over response for photon energies between 25-50 keV [8].

Calcium Sulphate doped with dysprosium ($CaSO_4$:Dy) is a highly sensitive thermoluminescent (TL) dosimeter material. It is approximately 30 to 50 times more sensitive than TLD – 100. This is especially true for ($CaSO_4$: Dy) exposed to gamma irradiation [41]. Dysprosium activated $CaSO_4$ commercially available as TLD-900 from the Harshaw-Bicron Chemical Co. The preference for this material is frequently justified by its easy preparation, high sensitivity, and apparently simple glow curve structure. $CaSO_4$: day compared to other phosphor shows small fading of the TL dosimetric peak [42]. By several studies it has been demonstrated that the TL glow curve behavior of $CaSO_4$:day and other phosphors are highly dependent on radiation quality and dose.

The main emission from the dye-doped version of this material is at 475 nm and 575nm. Longer wavelength emission is absorbed at 660nm and 750nm. The dose response of the main TL peke 220 °C from $CaSO_4$: Dy is linear up to a dose of (10Gy), after which it is superliner up to its saturation dose of (10^4Gy). High dose can be followed (up to 10^5Gy) using the high temperature TL peke (450ºc) [43] unusually the degree of super linearity is dependent upon the grain size in powdered $CaSO_4$ possibly related to self-absorption effects. The sensitivity is dependent upon the concentration of the dye and optimum values lead to minimum measured doses of 2 μGy for $CaSO_4$: Dy [8].

4.2 Experimental Procedure and Equipment's

Before next irradiation, the samples were first annealed to wipe any remaining information and then cool rapidly in the air at (75 ^oC/min) to the temperature of the room. For this reason annealed sample of the $CaSO_4$:Dy (TLD-900) at (400 ± 1 ^oC) for thirty minutes. All the treatments of annealing with specially designed oven of microprocessor controlled electrical which is able to control the temperature within (± 1.0 ^oC). The samples were irradiated at room temperature with beta rays from a

calibrated ^{90}Sr-^{90}Y source. The β-source activity is about (100 mCi). It is calibrated by the manufacturer on March, 10, 1994. The recommended working lifetime is about fifteen years. Strontium–90 emits high energy beta particles from their daughter products (^{90}Sr β-0.546 MeV together with ^{90}Y β-2.27 MeV). Beta radiation is absorbed by air, so its intensity reduced with distance much more quickly than inverse square law calculations would indicate.

The maximum range of ^{90}Y beta particles in air is approximately 9 meters. The typical strength of a 100 mCi ^{90}Srβ-source installed in a 9010 Optical Dating System is 2.64 Gy/minute=0.0438 Gy/Sec for fine grains of aluminium, or 3.3 Gy/min=0.055 Gy/sec for 100 m quartz on stainless steel. The equipment of irradiation is an additional part of the 9010 Optical Dating System which is purchased from Little More Scientific Engineering, UK [51] . The irradiated samples were read out by a reader of Harshaw QS 3500 manual type that is connected to a PC where studied and analyzed the signals of thermoluminescence. It always has been installed the standard filter of clear glass in the reader between the planchet and photomultiplier tube to eliminate the emitted infrared lights from the reader plus samples. All functions are divided between the reader and the specialized software Shell of the TLD that are running on the computer. All data storage, instrument control, and operator inputs are performed on the PC. Signal acquisition and conditioning are performed in the reader. As such, and can be analyzed each glow curve by using a best fit computer program depends on a procedure of a Marquardt algorithm minimization, related to expressions of the first-order and general order kinetics. The individual peaks present in the curve are resolved by the program, giving the best values for the parameters of different peak . The instrument includes a sample change drawer for inserting and removing the TLD elements. The reader uses contact heating with a closed loop feedback system which produces adjustable linearly lifted temperatures from 1 ^{o}C to 50 ^{o}C per second accurate to within ± 1 ^{o}C to 400 ^{o}C in the standard reader.

Figure 4.1 (a) the oven, (b) irradiation part, (c) TLD reader

CHAPTER 5

EXPERIMENTAL RESULTS

In this study the dose response behavior of ($CaSO_4$:Dy) (TLD-900) has been investigated at different linear heating rates between 1 $^{\circ}$C and 10 $^{\circ}$C by using the dose response function f(D). (TLD-900) crystal chips was firstly annealed at 400°C for 30 minutes before following irradiation and then cooled in air to room temperature. (TLD-900) wear irradiated immediately after the standard annealing at room temperature with β rays from a ^{90}Sr- ^{90}Y source (≈0.04 Gy/s).

Heating rate is one of the basic requirements for readout of thermoluminescence dosimeters (TLD) in studying the dosimetric parameters. Controlled heating is also a basic requirement for readout of thermoluminescence dosimeters (TLD).Therefore, heating rate becomes an important parameter in studying the dosimetric characteristics. Gorbics et al [52] were the first to draw attention to the effect of heating rate on the TL response. They attributed the reduction in TL response with increasing heating rate to thermal quenching of luminescence in TLD. [53-55]. Figure 5.1 depicts one of the deconvulated glow curve of TLD-900 using the computer glow curve deconvulation method [56] at a linear heating rate of 1 oC/s. The structure of the glow curve can be best described by three (P1, P2 and P3) first-order glow peaks. In this study the effect of the heating rate on the dose dependence of the main dosimetric peak (P2 at ≈280 ^{o}C) and on the total peak area of the glow curves of CaSO4: Dy (TLD-900). Was investigated in detail at different linear heating rates between 1 ^{o}C/s and 10 ^{o}C/s. Typical glow curves of TLD-900 sample, using a linear heating rate between 1 ^{o}C and 10 ^{o}C are shown in Figure 5.2a-5.2f

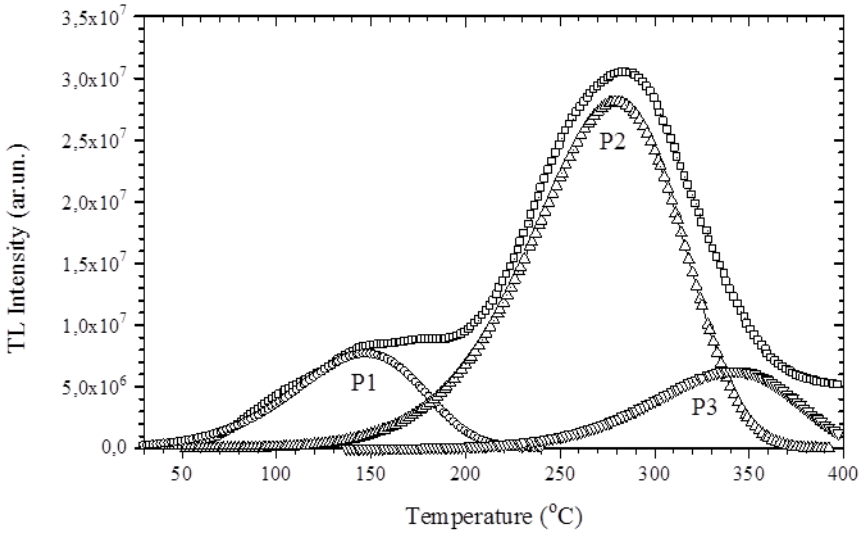

Figure 5.1The CGCD analyzed glow curves of CaSO4: Dy measured after 36 Gy irradiation with 90Sr-90Y beta source at room temperature. (FOM: 3.4%).

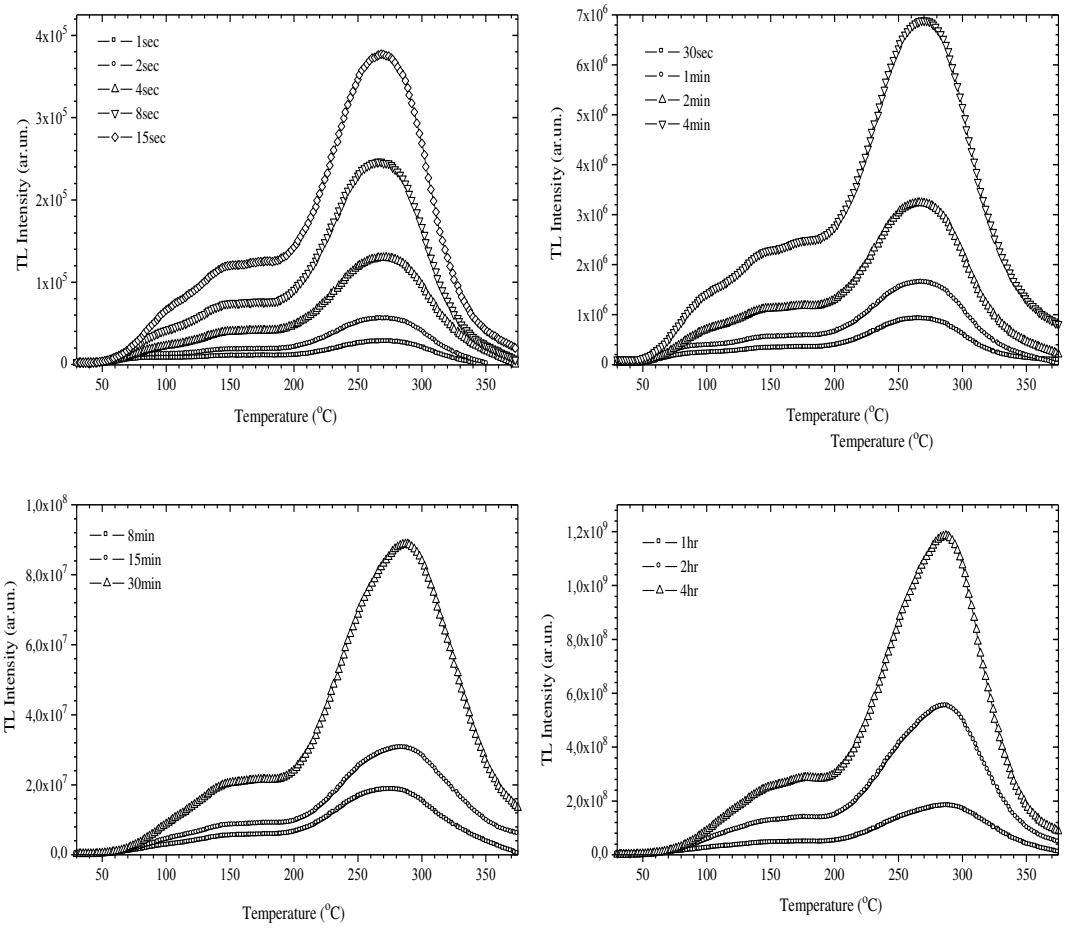

Figure 5.2a.Typical glow curves of TLD-900 exposed to beta rays from 0.04Gy up to 576 Gy and readout at linear heating rates of $\beta = 1\ ^{\circ}C/s$

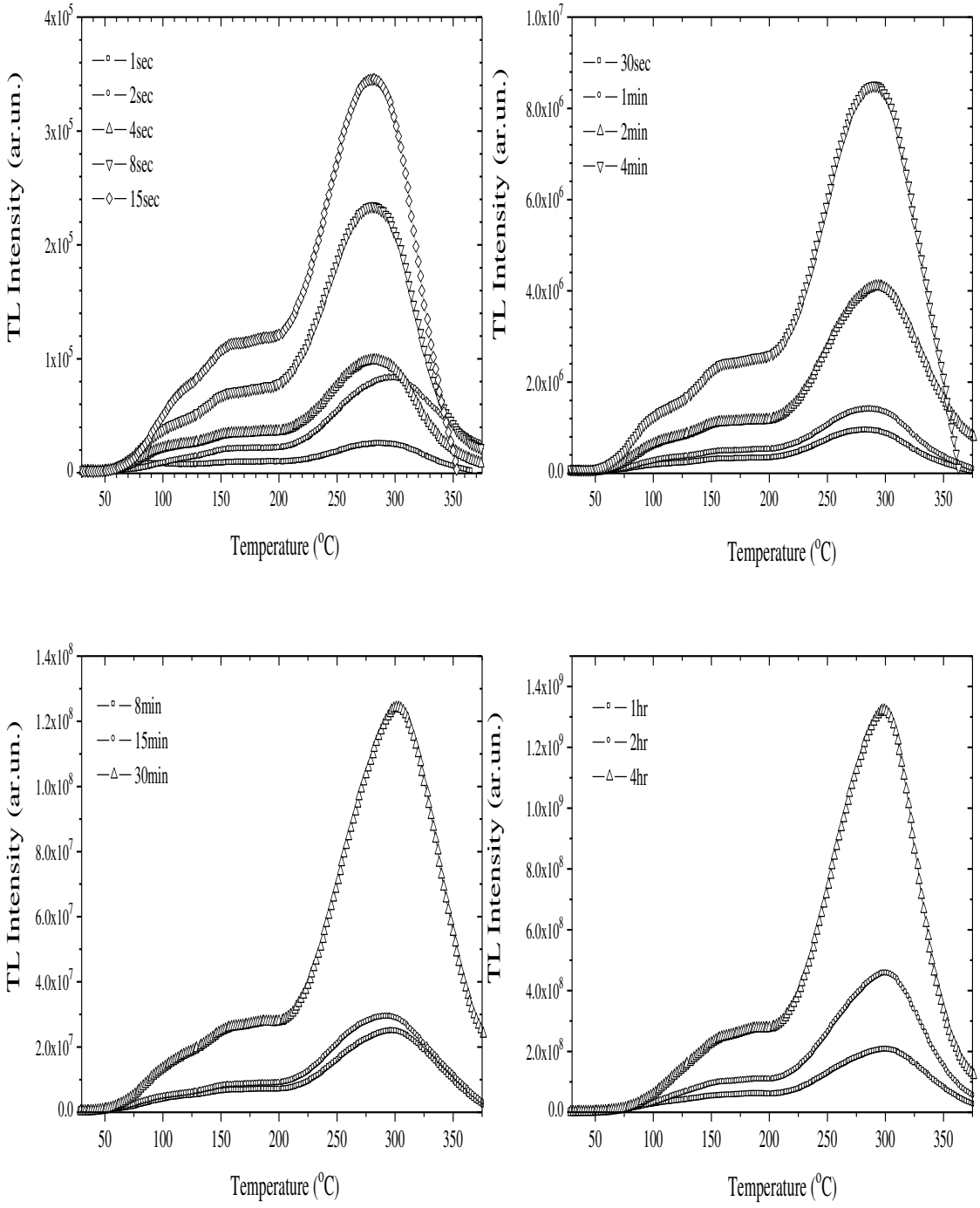

Figure 5.2b.Typical glow curves of TLD-900 exposed to beta rays from 0.04 Gy up to 576 Gy and readout at linear heating rates of $\beta = 2\ ^{\circ}C/s$

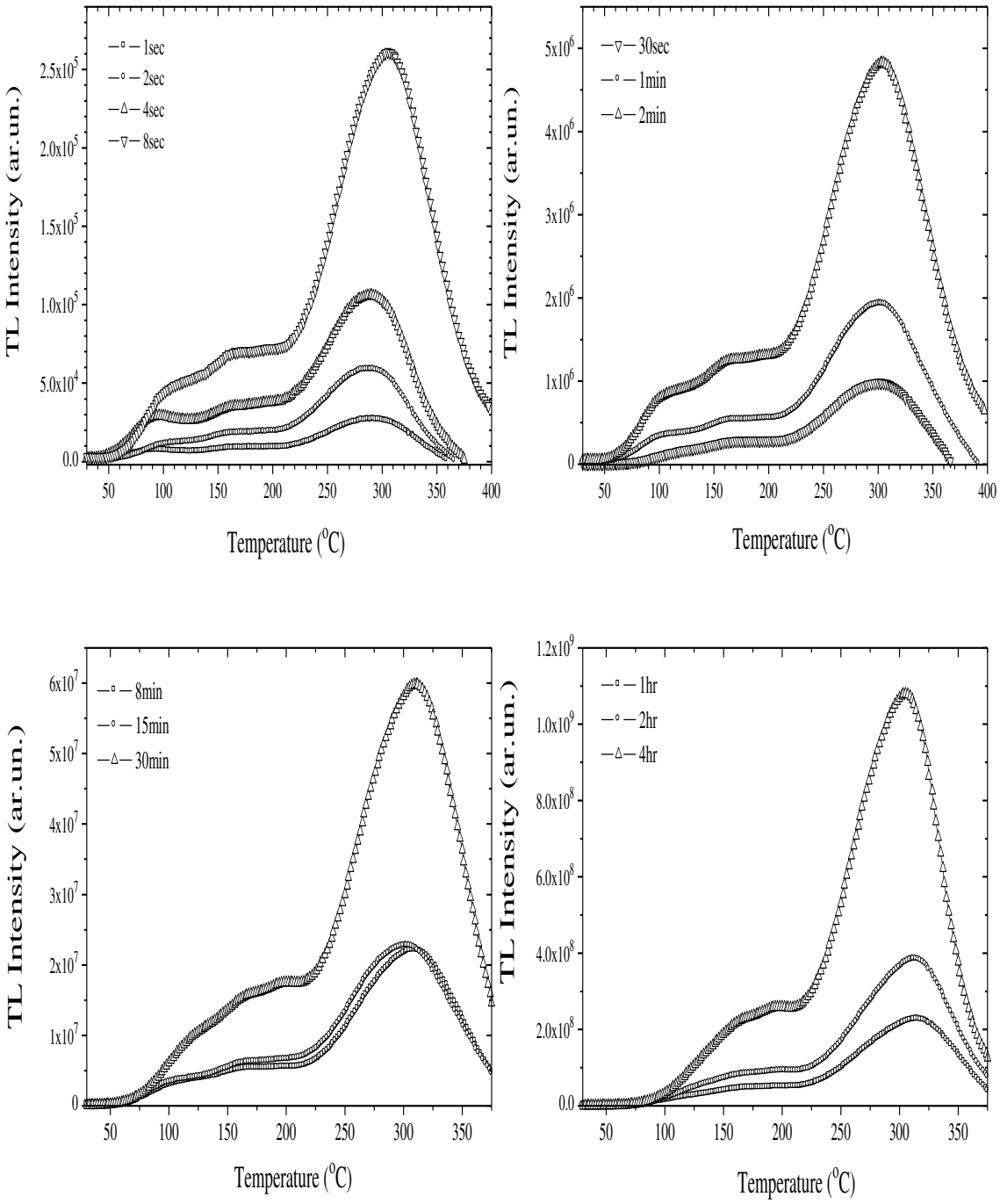

Figure 5.2c. Typical glow curves of TLD-900 exposed to beta rays from 0.04 Gy up 576 Gy and readout at linear heating rates of $\beta = 3\ ^{\circ}C/s$

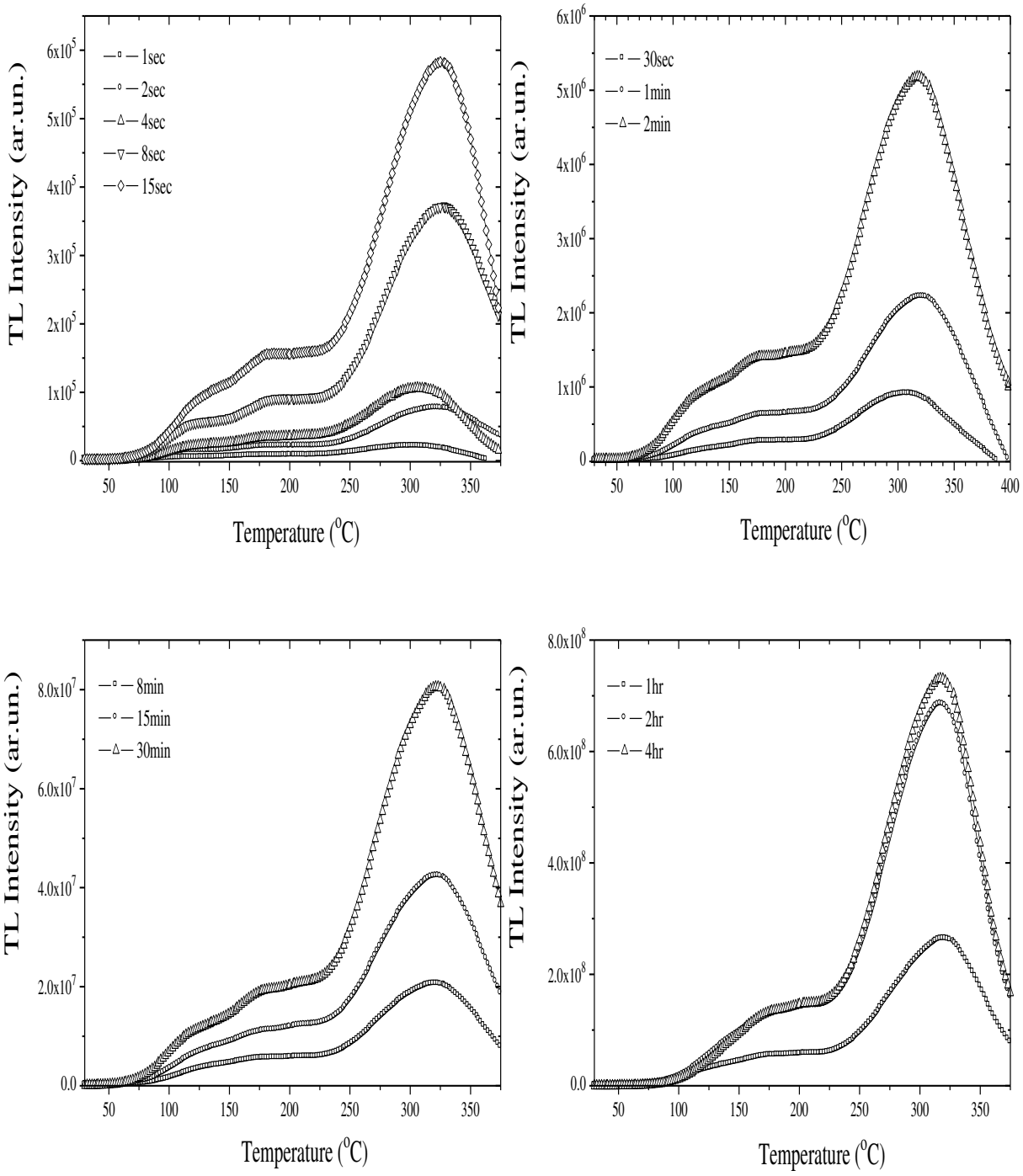

Figure 5.2d.Typical glow curves of TLD-900 exposed to beta rays from 0.04 Gy up to 576 Gy and readout at linear heating rates of $\beta = 5\ ^{\circ}C/s$

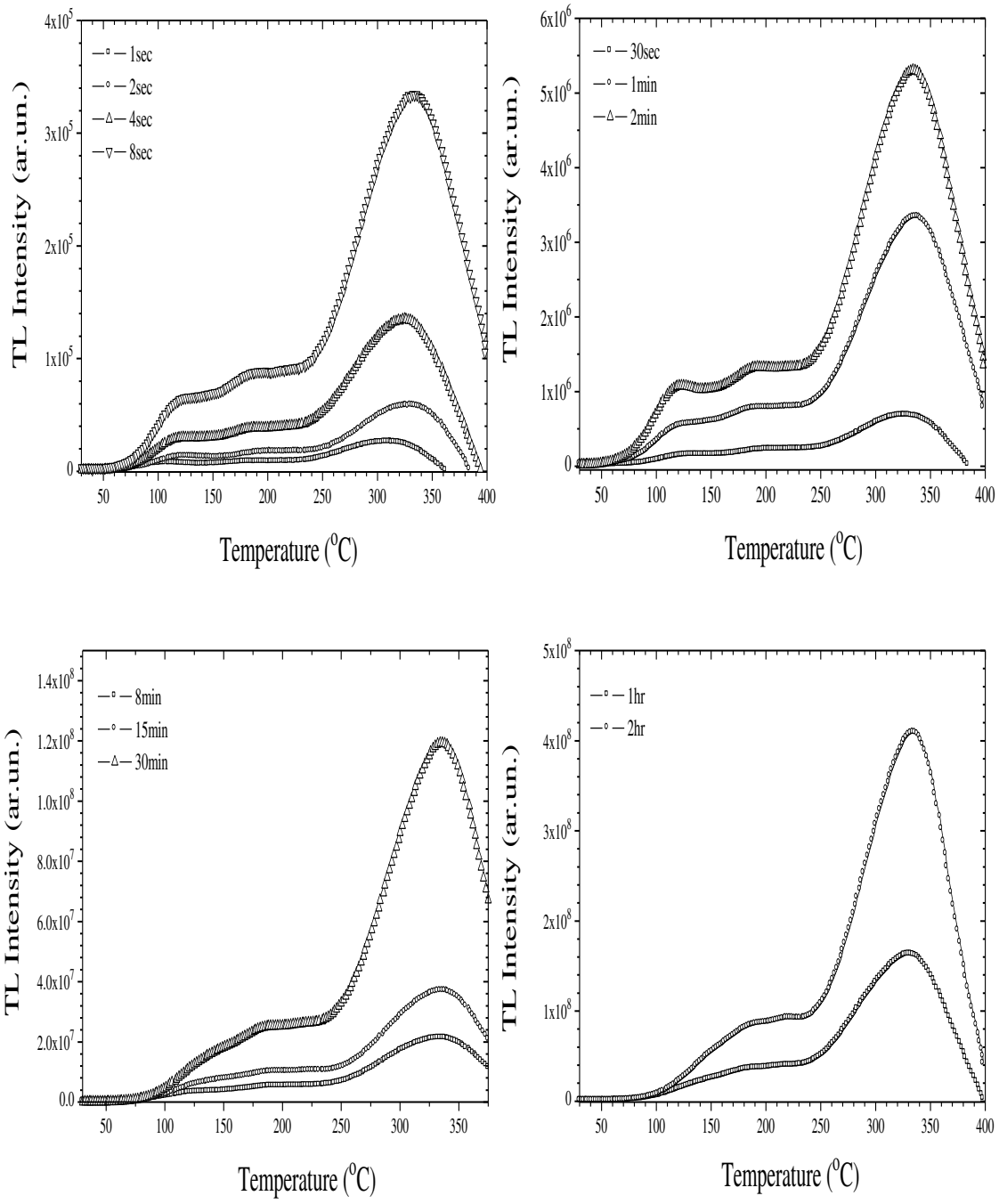

Figure 5.2e.Typical glow curves of TLD-900 exposed to beta rays from 0.04 Gy up to 576 Gy and readout at linear heating rates of $\beta = 7\ ^{\circ}C/s$

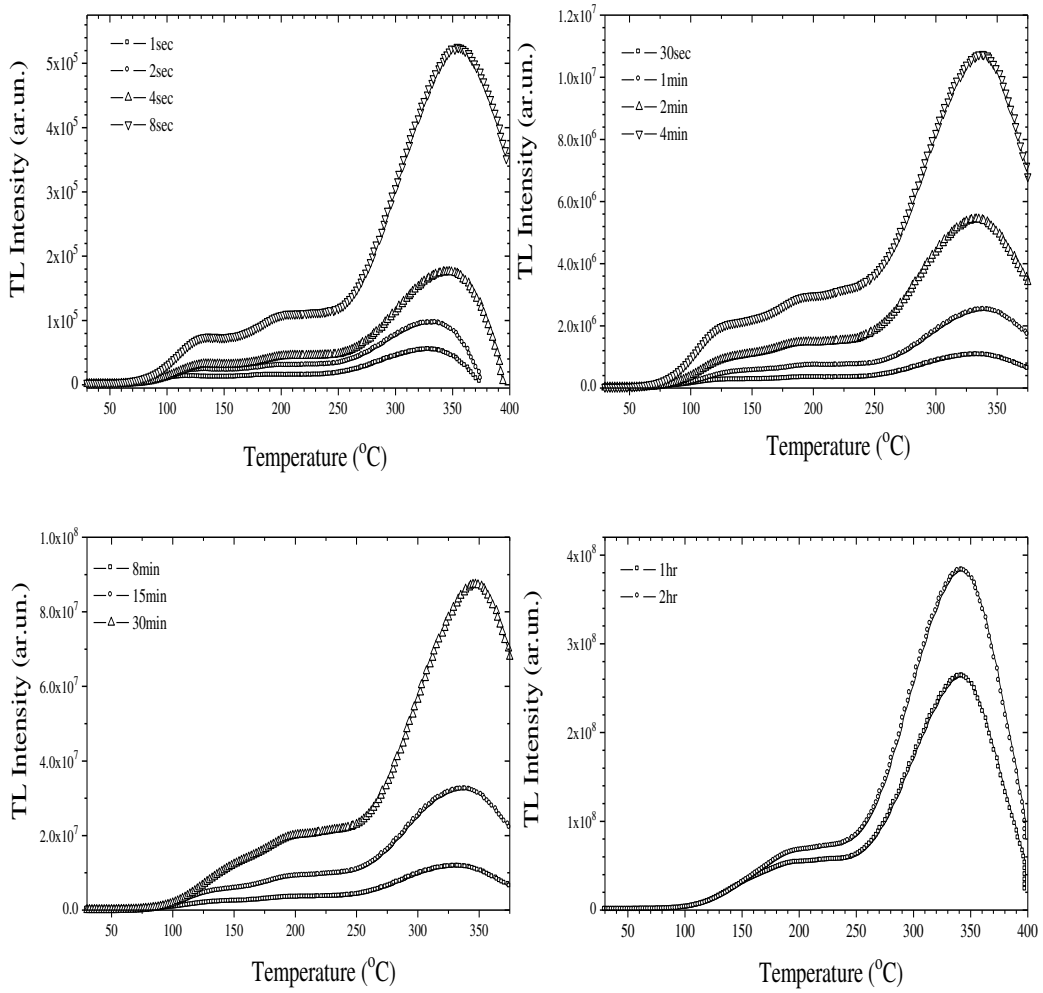

Figure 5.2f Typical glow curves of TLD-900 exposed to beta rays from 0.04 Gy up to 576 Gy and readout at linear heating rates of β = 10 °C/s.

In order to understand the effect of heating rate on the glow curves of TLD-900 different linear heating rates between 1°C/s and 10°C/s were applied. The measured and then normalized glow curves after different heating rates are shown in figure 5.3. As seen from this figure the peak temperatures of all peaks shifted to higher temperatures with increasing heating rate, and the total peak area of the glow curves decreases as the heating rate increases as expected in the theory. Figure 5.4 shows the growth of the height of the peaks as a function of dose. As seen from this figure, main glow peak (P2) of TLD-900 shows linear behavior up to 50 Gy for β=1 °C/s and 2 °C/s, the linearity of the glow peak continues up to 100 Gy for β=3 °C/s and 5 °C/s and the peak is linear nearly up to 10 Gy for β=7 °C/s and 10 °C/s.

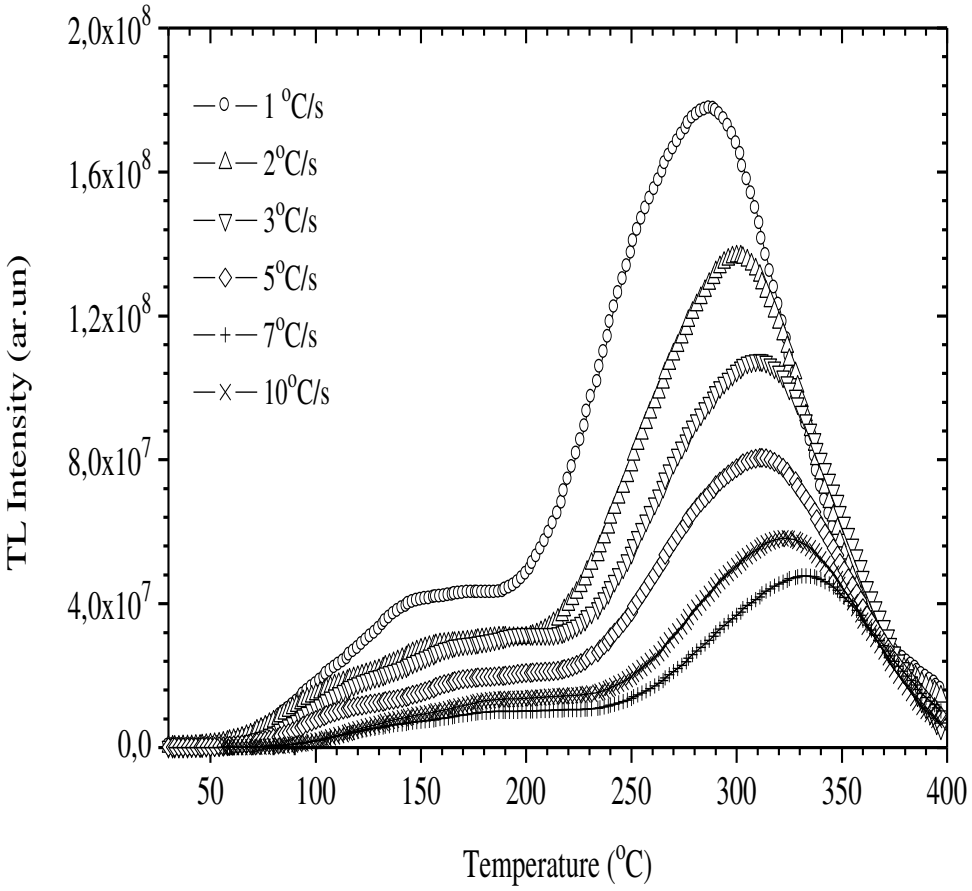

Figure 5.3 The glow curves of TLD-900 crystals irradiated (10 Gy) with ^{90}Sr-^{90}Y beta source at linear heating rates between 1 ^{o}C.s^{-1} and 10 ^{o}C.s^{-1}

Even figure 5.4 explains the growth of the height of the peaks as a function of dose, in order to understand the dose rate behavior of the peaks better, the dose response function, *f(D)* is evaluated by using equation 3.3 As seen from the figure 5.6, P2 exhibits the main characteristic of the dose response function. At linear heating rates of 1 ^{o}C/s and 2 ^{o}C/s the peak shows linear characteristic (*f(D)=1*) nearly up to 50 Gy, followed by a region of supralinear growth *(f(D)>1)*, the peak gradually goes into a region of sublinear growth *(f(D)<1)* near 10^3 Gy. For linear heating rates of 3 ^{o}C/s and 5 ^{o}C/s the peak shows linear characteristic (*f(D)=1*) nearly up to 100 Gy, after a region of supralinear growth *(f(D)>1)*, the peak gradually goes into a region of sublinear growth *(f(D)<1)* near 10^3 Gy. The dose response characteristic of the P2 shows linear behavior (f(D)=1) only at low doses then the peak saturates and goes into a region of sublinear growth (f(D)<1) after this dose.

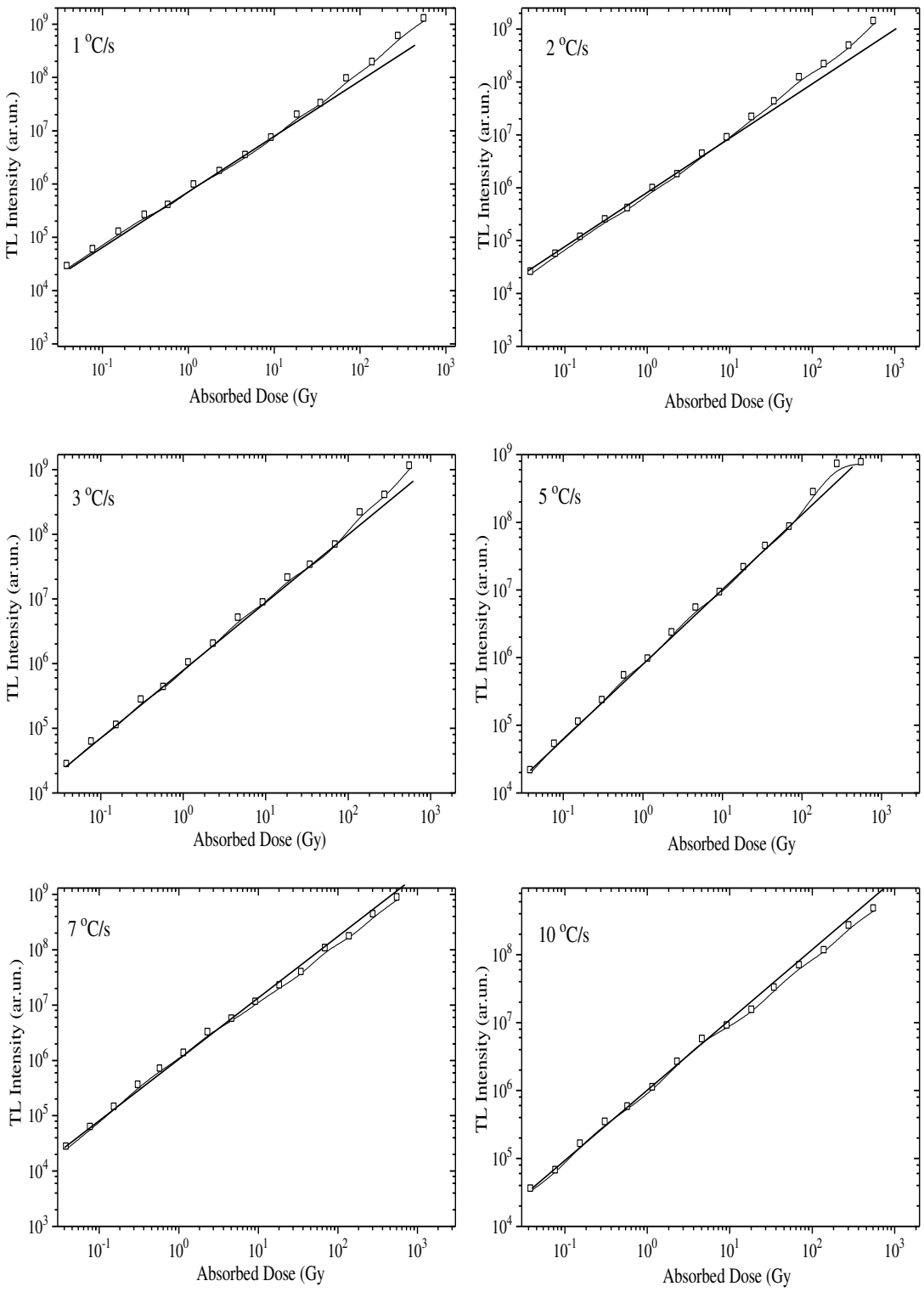

Figure 5.4 The growth of the height of the peaks from TLD-900 as a function of dose at a linear heating rate of β = 1 °C/s, 2 °C/s, 3 °C/s, 5 °C/s, 7 °C/s, 10 °C/s.

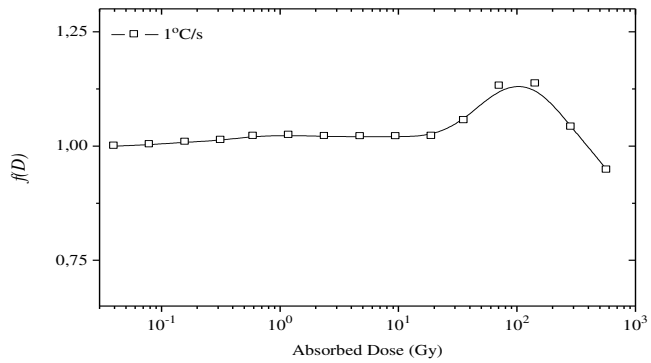

Figure 5.5a.The dose response function f(D) vs D of TLD-900 β=1°C/s.

As shown from figure 5.5a, the main glow peak ,p2, of TLD-900, namely linear (f(D)=1) region up to 10^2 Gy, followed by a region of supralinear growth (f(D)>1), gradually going into a region of sublinear growth (f(D)<1) after 10^3 Gy for the heating rate of 1 °C/s.

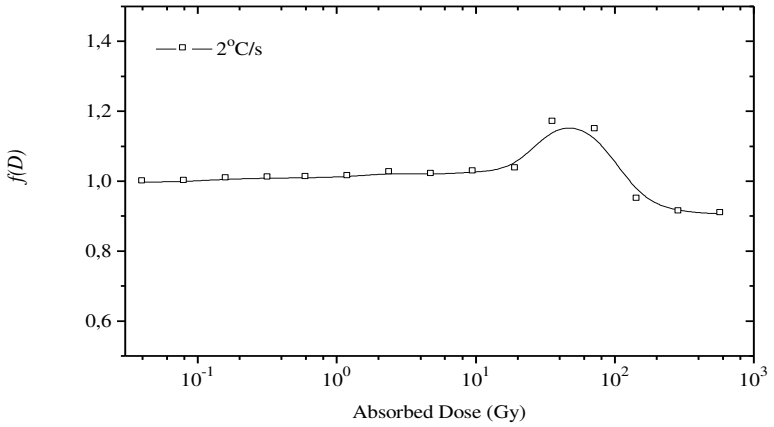

Figure 5.5b. The dose response function f(D) vs D of TLD-900 β=2°C/s.

As shown from figure 5.5b, the main glow peak,p2, of TLD-900, namely a linear (f(D)=1) region up to 10Gy to 10^2 Gy, followed by a region of supralinear growth (f(D)>1), gradually going into a region of sublinear growth (f(D)<1) after 10^3 Gy for the heating rate of 2 °C/s.

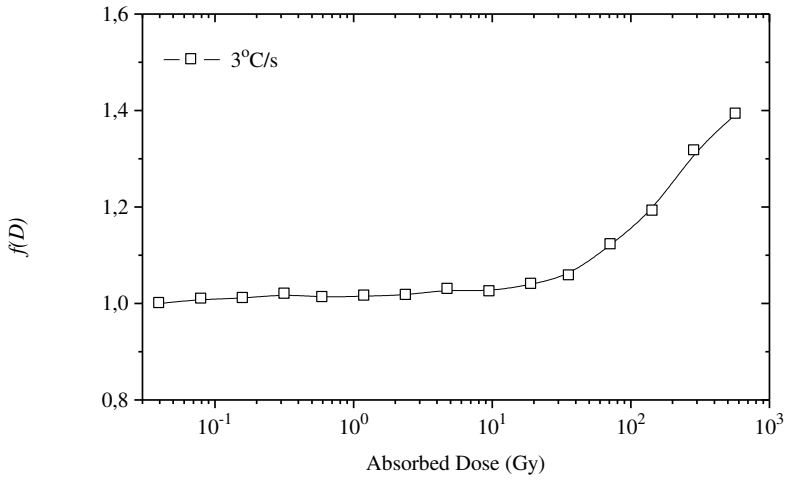

Figure 5.5c. The dose response function f(D) vs D of TLD-900 β=3°C/s.

As shown from figure 5.5c, the main glow peak, p2, of TLD-900, namely a linear (f(D)=1) region up to 10^2 Gy, followed by a region of supralinear growth (f(D)>1), gradually going into a region of sublinear growth (f(D)<1) after 10^4 Gy for the heating rate of 3 °C/s

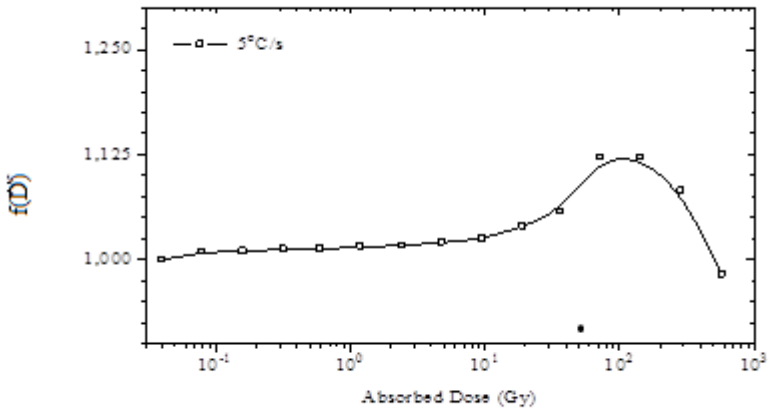

Figure 5.5d The dose response function f(D) vs D of TLD-900 β=5°C/s.

As shown from figure 5.5d, the main glow peak,p2, of TLD-900, namely a linear (f(D)=1) region up to 10 Gy, followed by a region of supralinear growth (f(D)>1), gradually going into a region of sublinear growth (f(D)<1) after 10^3 Gy for the heating rate of 5 °C/s

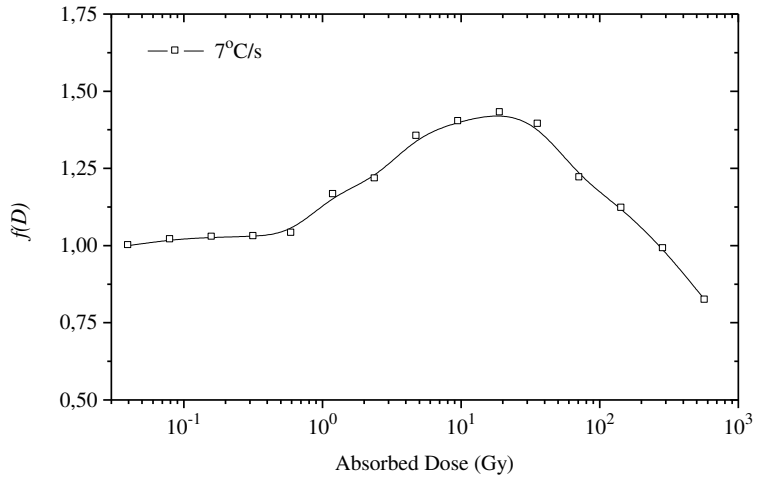

Figure 5.5e. The dose response function f(D) vs D of TLD-900 β=7°C/s.

As shown from figure 5.5e, the main glow peak,p2, of TLD-900, namely a linear (f(D)=1) region up to 10 Gy, followed by a region of supralinear growth (f(D)>1), gradually going into a region of sublinear growth (f(D)<1) after 10^2 Gy for the heating rate of 7 °C/s.

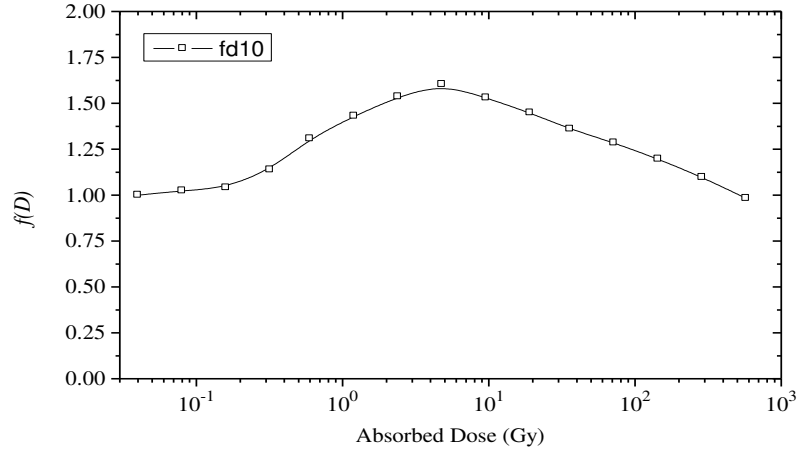

Figure 5.5f.The dose response function f(D) vs D of TLD-900 β=10°C/s.

As shown from figure 5.5f, the main glow peak,p2, of TLD-900, namely a linear (f(D)=1) region up to 10 Gy, followed by a region of supralinear growth (f(D)>1), gradually going into a region of sublinear growth (f(D)<1) after 10^3 Gy for the heating rate of 10 °C/s.

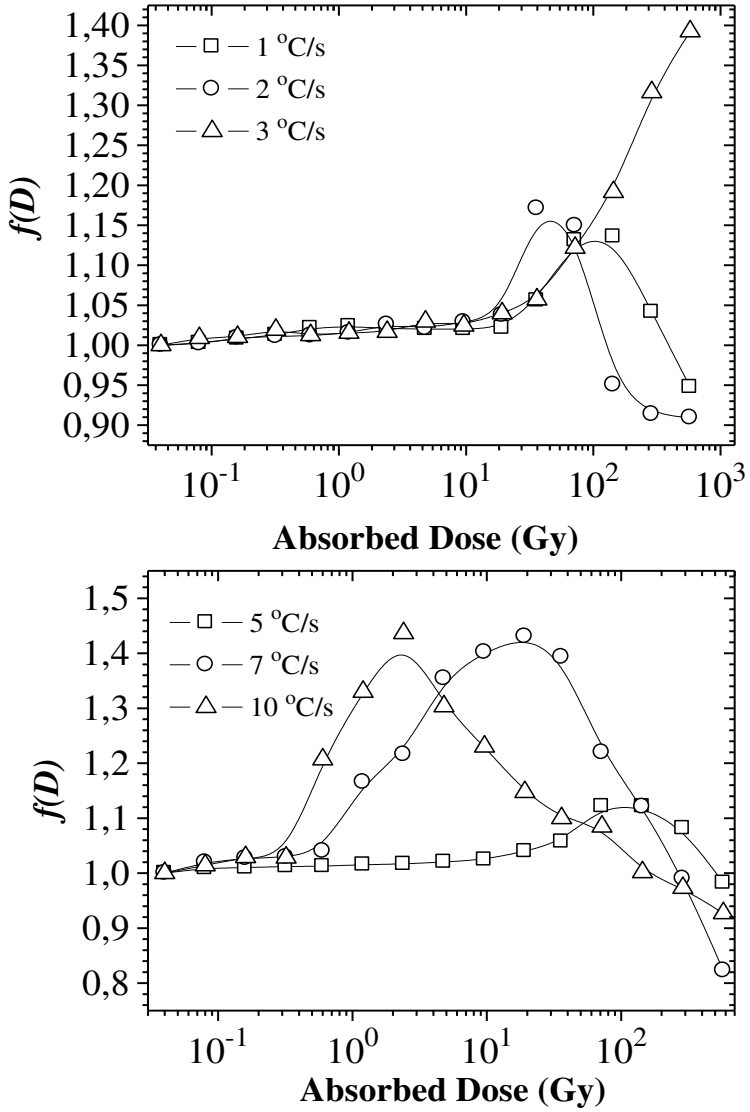

Figure 5.6. The dose response function f(D) vs D of TLD-900 at different linear heating rates.

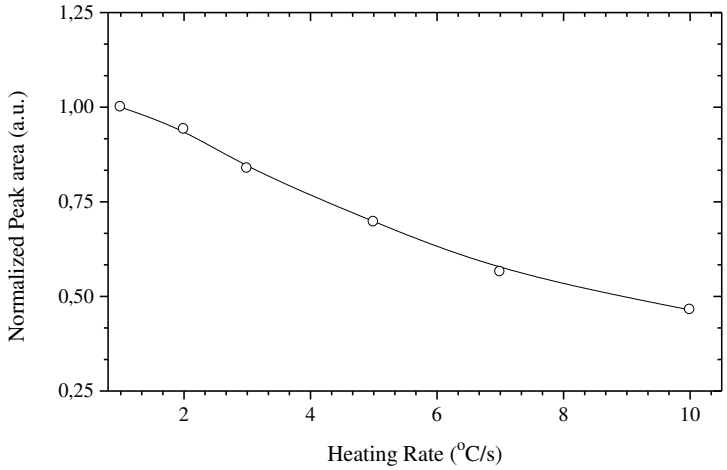

Figure 5.7 The change of the normalized total TL peak area of TLD-900 crystals irradiated with ^{90}Sr-^{90}Y beta source at linear heating rates between 1 °C/s and 10 °C/s.

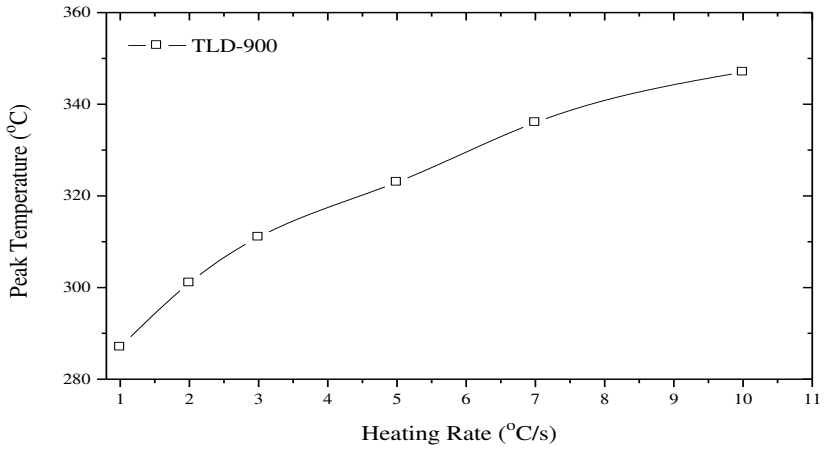

Figure 5.8 The change of the peak temperature TLD-900 crystals irradiated with ^{90}Sr-^{90}Y beta source at linear heating rates between 1 °C/s and 10 °C/s.

CHAPTER 6

CONCLUSION

The main objective of our study is an attempt to understand the effect of linear heating rate on the linearity and dose response characteristics of CaSO4: Dy by using the supralinearity index f(D). In order to have an idea about dose response characteristics of the glow curves, first of all the growth of the height of the peaks as a function of dose have been investigated at different linear heating rates between 1° C/s and 10 °C/s.

Further study, the dose response characteristics of the main dosimetric peak (P2) of TLD-900 have been investigated after different linear heating rates between 1 and 10 ^{o}C/s It is well known that a number of materials have characteristic dose response property. That is, an initial linear range is followed by a nonlinear (i.e. superlinear) region before saturation effects set in [56]. The nonlinear behaviors of glow peaks are well understood by using the supralinearity index *f(D)*. The experimental results of this study have shown that the linearity of the P2 continues nearly up to 100 Gy at heating rates of 3 ^{o}C/s and 5 ^{o}C/s. The results of the heating rate experiments shown that, the peak temperatures of all peaks are shifted higher temperatures and the integrated peak area of the curves decreases by about 50% as the heating rate increases as expected in theory. It is well known that the peak temperature of a TL peak depends on the heating rate. That influences the TL sensitivity and, hence, the trends of the dose-response curve [57]. Therefore, the controlled heating during the TL readouts is an important requirement to avoid the effects of heating rate. For the reduction of TL response at higher heating rates, the shift of the glow peak to higher temperature could result in increasing the probability of non-radiative transitions to compete with radiative transitions for luminescence emission and thus reducing the response by the way of thermal quenching.

Nonlinearities often occur in the dose dependence of thermoluminescence (TL). These include sublinearity; usually have an approach to saturation in the dose dependence, as well as supralinearity, also termed superlinearity in the literature.

Different researchers suppose in the field were considered have viewed the effect of supralinearity from two somewhat different points of view. The first point of view has to do with the rate of change with dose of the dose dependence function.

The other approach is related more to the applications of TL in the dosimetry and archaeological and geological dating, and essentially has to do with the correction to be made in extrapolation in cases where supra (super) linearity occurs following an initial linear dose range or prior to such a linear range. The effect of heating rate on the glow curves can be best described by the effect of thermal quenching. It is well known that the dosimetric characteristics of many TL materials are influenced by changes in location, size and shape of the glow curves due to changes in the heating rate. Thermal quenching was understood to be due to the increased the probability of non-radiative transitions competing with radiative transitions.

As seen from figures 5.6 the peak temperatures of all peaks are shifted higher temperatures when the heating rate increases as expected in theory. It is also seen from figure 5.7 the total peak area of the glow curves decreases as the heating rate increases.

REFERENCES

[1] Herman Cember and Thomas Eohnson (2009). Introduction To Health Physics (Fourth Edition).

[2] Chen, R. McKeever. S. (1997). Theory of Thermoluminescence and Related Phenomena. World Scientific Publishing Co. Pte. Ltd., Singapore.

[3] Mihaltsenko. G.A.(1967) Radiation physics.

[4] Schvarts. K.K. Grant. Z.A. (1974) Luminescent receivers and transformers of ionizing radiation. Proceedings of All-Union symposium. p. 94 (Moscow).

[5] Savikhin. F.A.(1974) Proceedings of inst. Of physics of est. Acad. Sci.

[6] Mckeever S.W.S. 1988 Thermoluminescence of solids. Cambridge: Cambridge university press.

[7] Othman I E and Charles M.W. (1999) thermoluminescence properties of novel thin clear fused quartz dosemeters, *Radiation Protection Dosimetry*

[8] M.G.Guelev. I.T. Mischev. B.Burgkhardt and E.Piesch, (1994). *Radiation Protection Dosimetry*.51 -35.

[9] McKeever, S. Moscovitch. M. Townsend. P. (1995) Thermoluminescence Dosimetry. Materials: Properties and Uses Nuclear Technology Publishing. England.

[10] Furetta. C.(2003) Handbook of thermoluminescence. World scientific publishing co. Pte. Ltd. singapore.

[11] Schauer, D. Brodsky. A. Sayeg. J.(2003) Handbook of radioactivity analysis, second edition. Academic press.

[12] Vasilis Pagonis. George Kitis and Claudio Furetta. Numerical and exercises in thermoluminescence.

[13] J.T. Randall and M.H.F. Wilkins (1945), Phosphorescence and electron traps. The study of trap distributions, *proc.r.soc.london ser. A*, 184, 366.

[14] Y.Horowitz. (1984). Thermoluminescent Dosimetry in Thermoluminescence and Thermoluminescent Dosimetry Vol.II, CRC Press Boca Raton F1.

[15] Lakshmanan. A.R. Madhusoodanan, U. 1998. Behaviour of

CaSO4:Dy embedded Teflon discs at high annealing temperatures

Radiation Measurements. 29 (5), 527–530.

[16] G.F.J. Garlick and A.F. Gibson (1948). The Electron Trap Mechanism of Luminescence in sulphate and Silicate Phosphors, *Proceedings of the Physical Society.* **60**, 574,.

[17] May, C.E And Partridge. J,.A.(1964). Thermoluminescence kinetics of alpha irradiated alkali halides. *Journal of chemical physics*, **40**. 1401-1415.

[18] T S C Singh. P S Mazumdar and R K Gartia(1988) on the determination of activation energy in thermoluminescence by the initial rise method J. *Phys. D: Apply. Phycics.*

[19] Petrov S.A and Bailiff I.K. (1997) Determination of trap depths associated with Tl peaks in syntheic quartz (300-550k). *Radiation Measurem*ents. 27-185

[20] Mahua Karmakar (2012) on the Initial Rise Method for Kinetic Analysis in Thermally Stimulated Luminescence

[21] Aramu F. Brovetto P. and Rucci. A (1966), Activation energy in the NaCl thermoluminescence. *Physics Letters*. Vol.23, pp.308-309

[22] K H Nicholas and J Woods (1964). The evaluation of electron trapping parameters from conductivity glow curves in cadmium sulphide. Br. *Journal of Physics D: Applied Physics* 15 783.

[23] S C Singh. P S Mazumdar and R K gartia.(1990). A critical appraisal of methods of various heating rates for the determination of the activation energy of a thermoluminescence peak. *Journal of Physics D: Applied Physics.* **23** 562

[24] Bohun, A. (1954). Thermo emission und photoemission von Natrium chlorid.

Czech. *Journal of Physics*. 4, 91-93

[25] I.A. Porfianovitch, (1954). Proceedings of the 11th international conference on solid state Dosimetry, *Journal of Experimental and Theoretical Physics.* Ussr *26 - 696.*

[26] A.h. Booth (1954). Separation of p^{32} from neutron-irradiated sulphur. *Canadian Journal of Chemistry*. 32 -214.

[27] W. Hoogenstraaten,. (1958). A method of measuring specific resistivity and hall effect of discs of arbitrary shape. *Philips Research Report*, t. 13 - 515.

[28] R. Chen and S.A.A. Winer, (1970) Effects of Heating Rateson Glow Curves, *Journal of Physics D: Applied Physics*. 41, 5227-5232.

[29] R.K. Gartia, S. Ingotombi, T.S.G. Singh, and P.S. Mazmudar, (1991) on the determination of the activation energy of a thermoluminescence peak by the two-heating-rates method. *Journal of Physics D: Applied Physics*.24 - 65, **12**.

[30] Grossweiner. L.I. (1953). A note on the Analysis of First-Order Glow curves. *Journal of Applied Physics*, **24**, 1306-1308.

[31] R. Chen, (1969) on the Calculation of Activation Energies and Frequency Factors from Glow Curves *Journal of Physics D: Applied Physics*. 40 -570.

[32] Halperin, A. and Braner. A. (1960). Evaluation of thermal activation energies from glow curves. *Physical Review Letters*, **117**, 408-415.

[33] Yamashita ,T,Nada,N, Onishi,H. and Kitamura, S (1968).In, Proc.and Conf. on Luminescence Dosimetry Gatlinburg ,Conf 680920,p,4.

[34] Azorin, J., Furetta, C., and Scacco, A. (1993) Preparation and properties of thermoluminescent materials," *Physics Stat. Solids*

[35] Ingle, N.B. Omanwar, S.K., Muthal. P.L. Dhopte. S.M., Kondawar, V.K. Gundurao. T.K. Moharil, S.V. 2008. Synthesis of CaSO4:Dy, CaSO4:Eu3 þ and CaSO4:Eu2 þ phosphors. *Radiation Measurements*. 43, 1191–1197.

[36] Numan. Salah. Share. P.D. Lochab. S.P. Kumar. Pratik, 2006. TL and PL studies on CaSO4:Dy nanoparticles. *Radiation Measurements* 41, 40–47.

[37] Aypar. A. 1978. Studies on thermoluminescent CaSO4:Dy for dosimetry. Int. *Applied Radiation and Isotopes*. 29, 369–372

[38] Chatterjee, S. Bakshi, A.K. Kinhikar R.A. Chourasiya. G. Kher. R.K. (2009). Response of CaSO4:Dy phosphor based TLD badge system to high energy electron beams from medical linear accelerator and estimation of whole body dose and skin dose. *Radiation Measurements*. 44, 257–262.

[39] Mathur, V.K. Lewandowski. A.C. Guardala, N.A. Price. J.L., 1999. High dose measurements using thermoluminescence of CaSO4:Dy. *Radiation Measurements*. 30, 735–738.

[40] Nunes. M.G. Campos. L.L. 2008. Study of CaSO4:Dy and LiF:Mg,Ti detectors TL response to electron radiation using a SW Solid Water phantom. *Radiation Measurements*. 43, 459–462.

[41] Yigal and Horowitz. Thermoluminescence and thermoluminescent dosimetry.

[42] Portal G. (1981) principal TL products in Applied Thermoluminescence Dosimetry.

[43] F.Hasan ,G. Kitis and S.Charalambous. (1985) *nucl. Instrum meth*. B 9 - 218.

[44] A. Halperin and R. Chen (1966), Thermoluminescence in Semiconducting Diamonds . *Physical Review Letters*. 148-839.

[45] R. Chen and S.W.S. McKeever. (1994), Characterization of Nonlinearities in the Dose dependence of Thermoluminescence. *Radiation Measurements* 23 - 667

[46] J.R.Cameron. N. Suntharalingam, and G.N. Kenney1968.*Thermoluminescent*

Dosimetry. The University of Wisconsin Press

[47] Furetta, C. Prokic, M. Salamon, R. Prokic, V. and Kitis. G.(2001) *Nuclear Instruments and Methods* A, 456, 411.

[48] S.G.E. Bowman and R. Chen. (1979) Superlinear Filling of Traps in Crystals Due to Competition During Irradiation. *Radiation Protection Dosimetry*

[49] R. Chen and G. Fogel. (1993) Superlinearity in TL Revisited, *Radiation Protection Dosimetry* 47 - 23.

[50] N. Kristianpoller, R. Chen, and M. Israeli. (1974). Dose Dependence of Thermoluminescence Peaks, *Journal of Physics D: Applied Physics*. 7 (1974) 1063.

[51] 9010 Optical Dating system User Manuel, Dec. 1993.

[52] Gorbics, S. G. Nash. A. E. and Attix F. H. (1969). Thermal Quenching of Luminescence in Six Thermoluminescent Dosimetry Phosphors. In: Proc. 2nd Int. Conf. on Luminescence Dosimetry, Gatlinburg. CONF 680920. pp. 587-608.

[53] Pradhan. A.S. (1996). Thermal Quenching and Two Peak Method –Influence of Heating Rates in TLD. *Radiation Protection Dosime*try, 65, 73-78

[54] Pradhan, A. S. and Bhatt. R. C. (1979). Influence of Heating Rates on the Response of TLD Phosphors. Int. Jornal *Applied Radiation and Isotopes* 30, 508-510.

[55] Kitis, G. Papadopoulos. J. S., Charalambous, S. and Tuyn, J. W. (1994). The Influence of Heating Rate on the Response and Trapping Parameters of a-Al2Os;C. *Radiation Protection Dosime*try. 55, 183-190.

[56] Bos, A.J.J., Piters, J. M., Gomez Ros, J. M. and Delgado, A. (1993). (GLACANIN. and Intercomparision of Glow Curve Analysis Computer Programs) IRI-CIEMAT Report 131-93-005 IRI Delft

[57] Kortov V.S., Milman I.I. Nikiforov S.V. Moiseykin E.V. Kondrashov S.V. (2007) *Radiation Measurements*. 42 590-593.